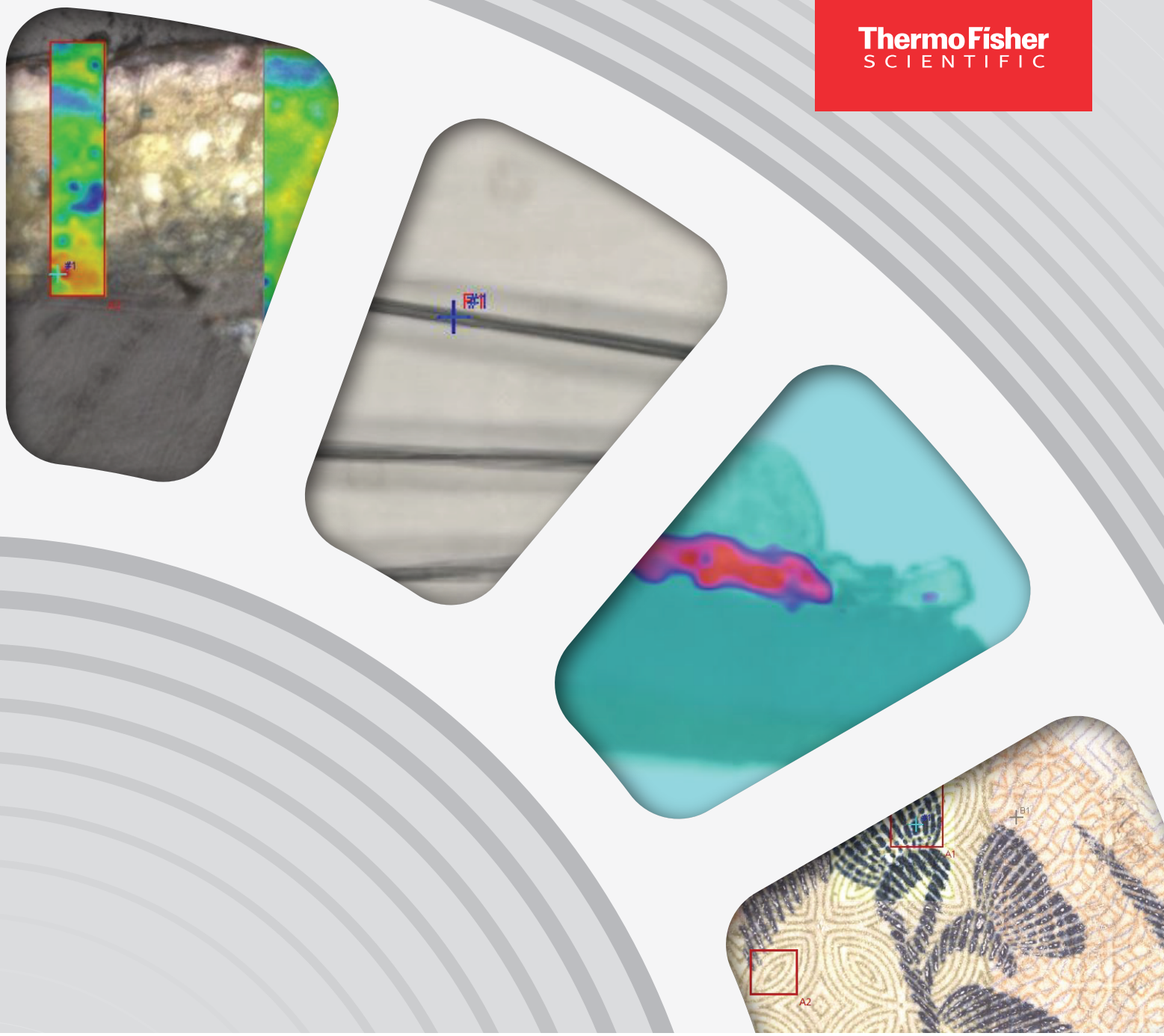

Forensic Analysis with Microspectroscopy Compendium

When what matters are microns and minutes

thermo scientific

Summary

These four application notes provide a cross-section of the uses of FTIR microscopy (and Raman microscopy in the busy forensics' laboratory).

We first examine paint chips where the layers provide clues to their origin. Next, a simple test reveals how a document was altered, shown by the different chemistry of inks. Moving to crime scenes, we find single fibers from a location are a common source of information about the scene; we examine natural and synthetic fibers. Finally, we return to paints, but in a historical setting with a sample from Venice, Italy, where we can tie the content of the layers to the specific habits of the painter.

These applications provide a taste of what the Thermo Scientific Nicolet RaptIR FTIR Microscope can be accomplished for labs where there is no knowing what sample will come next.

Contents

Summary	2
Investigating automobile paint chip layers with FTIR and Raman microscopy	4
Analyzing inks and toners with FTIR microscopy	9
Forensic analysis of fiber and hair using FTIR microscopy	13
Analysis of a Tintoretto stratigraphy with micro-FTIR spectroscopy	19



Application note

Investigating automobile paint chip layers with FTIR and Raman microscopy

Introduction

Forensic labs are often asked to piece together evidence from hit and run incidents where one of the vehicles involved has fled the scene. Evidence left behind can include fragments of glass, pieces of the bumper, headlights, or tail lamps, as well as skid marks and paint residues. Collisions between a vehicle and an object or person can result in the transfer of paint, either as chips or smears.

Automobile paint is often a complex mixture of various components applied in multiple layers. While this complexity presents a challenge for analysis, it also provides a wealth of potential information for vehicle identification. Fourier transform infrared (FTIR) and Raman microscopy are some of the critical techniques used to address this challenge and provide non-destructive analysis of individual layers within the total paint structure.

Paint chip analysis begins with the collection of spectral data, which can be directly compared to a control sample or used in conjunction with a database to identify the make, model, and year of the vehicle. One such database is the Paint Data Query (PDQ) Database, which is maintained by the Royal Canadian Mounted Police (RCMP). Access is available to forensic laboratories who participate in the program to maintain and grow the database. This application note will focus on the first step in the analysis process; collection of spectral data from paint chips using FTIR and Raman microscopy.

Paint chip sample preparation

FTIR data was collected using a Thermo Scientific™ Nicolet™ RaptIR™ FTIR Microscope; Raman data was collected using a Thermo Scientific™ DXR3xi Raman Imaging Microscope. The paint chips were obtained from damaged sections of an automobile; one paint chip is from a door panel, and the other is from a bumper. Embedding samples in epoxy resin is a common way to mount them for cross-sectioning, but there is a risk that the resin penetrates the sample and complicates the analysis. To avoid this, the paint chips were sandwiched between two sheets of poly(tetrafluoroethylene) (PTFE) while being cross-sectioned.

The paint chip cross-sections were manually separated from the PTFE prior to analysis and pieces were placed on a barium fluoride (BaF_2) window. FTIR mapping was done in transmission mode using the optimized 15x objective and condenser, a 10 x 10 μm^2 aperture, and 5 µm steps. The same samples were used for Raman analysis for the sake of consistency, even though it was not necessary to have thin cross-sections on BaF_2 windows. It should be noted that BaF_2 has a Raman peak at 242 cm^{-1} that can be observed as a weak peak in some of the spectra. This signal should not be attributed to the paint chips. Raman images were collected using image pixel sizes of 2 µm and 3 µm. Spectra were analyzed for key component peaks and compared to commercially available libraries by employing techniques such as multi-component searching to help with identification.

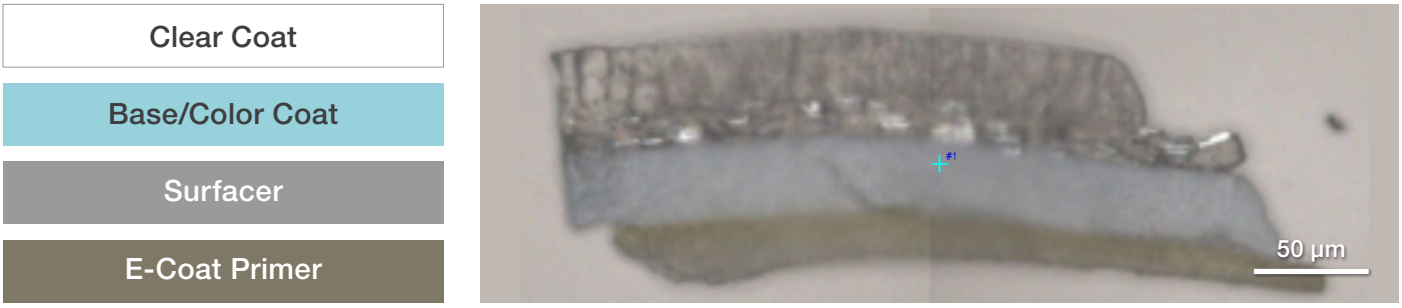

Figure 1. Schematic of a typical four-layer automobile paint sample (left). Video mosaic image of a paint-chip cross-section taken from the door of an automobile (right).

Automobile paint composition

While the number of layers in a paint chip can vary, samples typically have about four layers (Figure 1). The layer applied directly to the metal is an electro-coat primer layer (approx. 17-25 µm thick), which is used to protect the metal from the environment and to provide a surface for the subsequent paint layers to adhere to. The next layer is the surfacer layer (approx. 30-35 µm thick) that acts as an additional primer and provides a smooth surface for the paint layers that follow. Next, there is a basecoat or color coat (approx. 10-20 µm thick), which contains the primary pigments of the paint. The final layer is a clear coat (approx. 30-50 µm thick), which protects the paint layers beneath it and provides a glossy finish. Part of the challenge of analyzing trace paint evidence is that paint chips and smears will not always contain all the layers present on the source vehicle. Additionally, samples from other areas might have different compositions. For instance, a paint chip from a bumper may contain bumper materials as well as the finish.

FTIR paint chip analysis – automobile door

A visible image of the paint-chip cross-section is shown in Figure 1. Four layers can be seen in the visual image, corresponding to the four layers identified by infrared analysis. The whole cross-section was mapped, and individual layers were defined using FTIR images of different peak areas.

Representative spectra from the four layers and corresponding FTIR images are shown in Figure 2. The first layer is consistent with an acrylic clear coat and includes polyurethane, melamine (peak at 815 cm^{-1}), and styrene. The second layer is the base (color) coat and is chemically similar to the clear coat. It also consists of acrylic along with melamine and styrene. While they are similar, and no specific pigment peaks were identified, there are still differences in the spectra, mainly in peak intensities. The spectrum from Layer 1 has more intense peaks at 1700 cm^{-1} (polyurethane), 1490 cm^{-1}, 1095 cm^{-1} (C-O) and 762 cm^{-1}. The spectrum from Layer 2 has more intense peaks at 2959 cm^{-1} (methyl), 1303 cm^{-1}, 1241 cm^{-1} (ester), 1077 cm^{-1} (ester) and 731 cm^{-1}.

Spectra from the surfacer layer matched with library spectra of an alkyd based on isophthalic acid. The final electro-coat primer layer consists of an epoxy and, potentially, polyurethane. Overall, results are consistent with what is typically found in automobile paints. The analysis of the different components in each layer was performed using commercial FTIR libraries rather than automobile-paint-specific databases, so while matches are representative, they may not necessarily be exact. Using databases specifically designed for this type of analysis would improve identification and could even be used to determine the make, model, and year of the automobile.

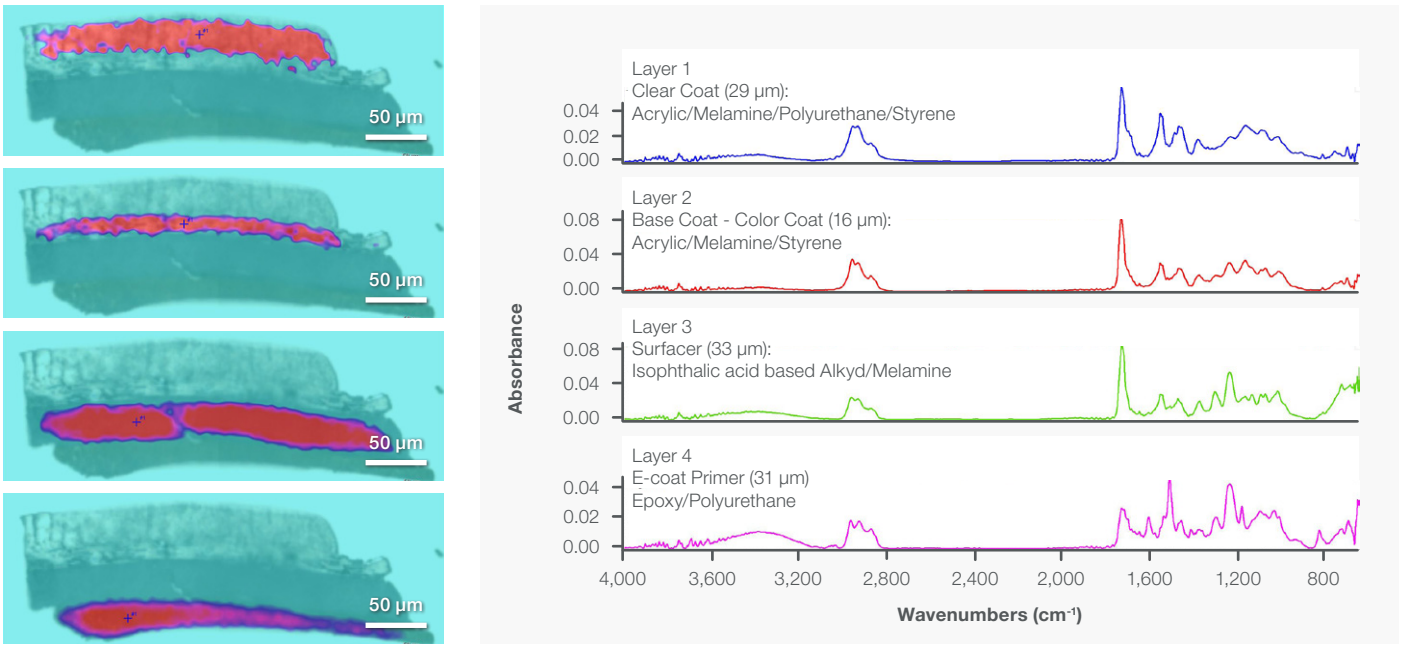

Figure 2. Representative FTIR spectra from the four identified layers in the door paint-chip cross-section. Infrared images are generated from peak areas associated with the various layers, which are then superimposed on the video images. The red areas show the location of the various layers. The infrared image covers an area of 370 x 140 µm² using a 10 x 10 µm² aperture and 5 µm steps.

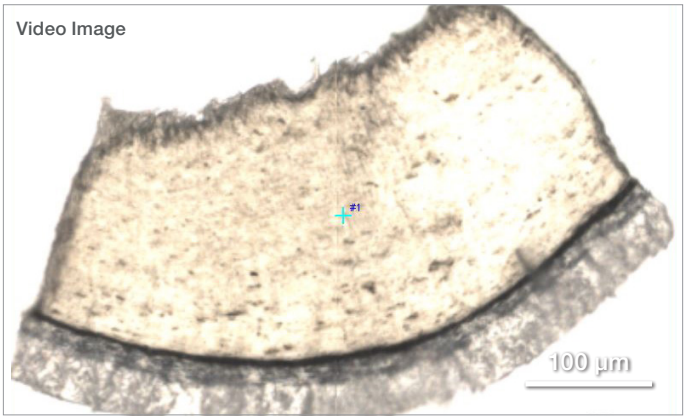

Figure 3. Video mosaic image of a paint-chip cross-section taken from the bumper of an automobile.

FTIR paint chip analysis - bumper

A video image of a bumper paint-chip cross-section is shown in Figure 3; at least three layers are clearly visible. Infrared images of the cross-section confirmed three distinct layers (Figure 4). The outer layer is a clear coat that appears to be a polyurethane material with acrylic, which matched with clear coat spectra from a commercial forensic library. While the spectrum from the base (color) coat is very similar to the clear coat, it was still distinct enough to be differentiated from the outer layer. There are significant differences in relative peak intensities. The third layer is likely the bumper material itself and consists of polypropylene as well as what appears to be talc. Talc can be used as a reenforcing filler with polypropylene to improve a material's structural properties. The two outer layers are both consistent with paint layers found in automobile paint, but no specific pigment peaks were identified in the base coat layer.

Raman microscopy

To gather additional information on the samples, cross-sections were also analyzed using a Raman imaging microscope. The Raman analysis was complicated by fluorescence from the samples. Several different laser sources (455 nm, 532 nm, and 785 nm) were tested to evaluate the balance between fluorescence and Raman signal intensity. For the door paint chip, a 455 nm laser gave the best results; while there was still fluorescence present, it could be compensated for with a baseline correction. This approach, however, did not work with the epoxy layer because the fluorescence was too extreme, and the material was sensitive to laser damage. While some lasers worked better than others, none were a practical choice for analysis of the epoxy layer. A 532 nm laser was used for the Raman analysis of the bumper paint-chip cross-section. There were still fluorescence contributions, but these were addressed with a baseline correction.

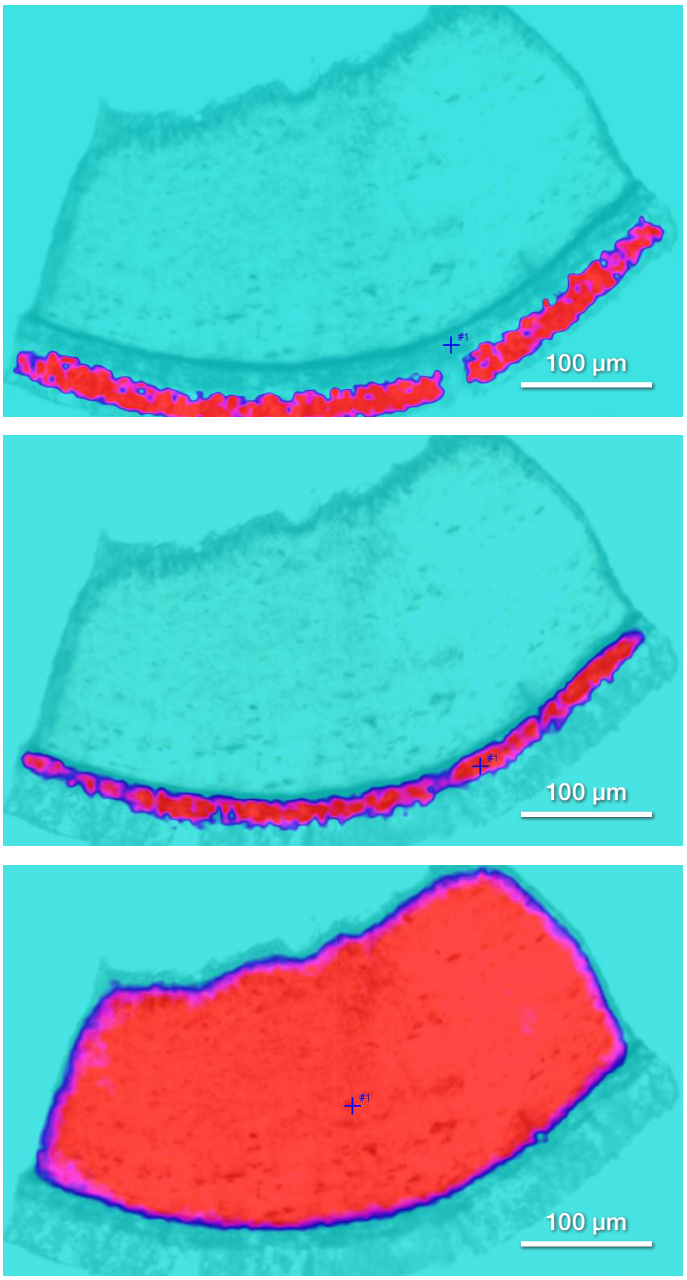

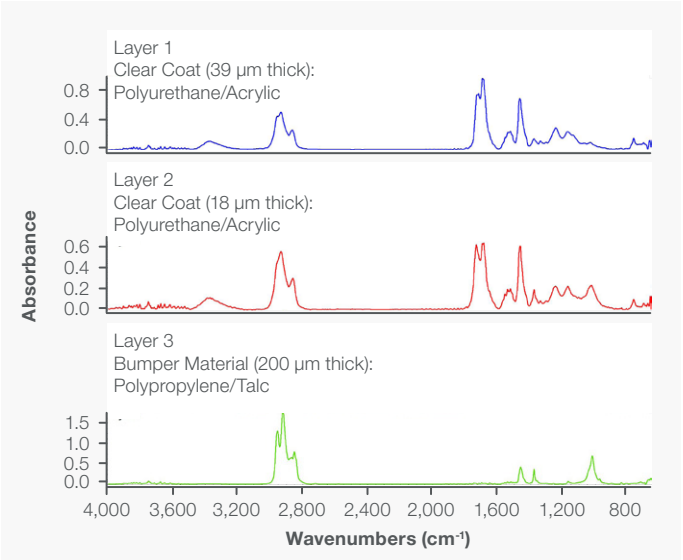

Figure 4. Representative FTIR spectra from the three identified layers in the bumper paint-chip cross-section. Infrared images are generated from peak areas associated with the various layers, which are then superimposed on the video images. The red areas show the location of the various layers. The infrared image covers an area of 535 x 360 µm² using a 10 x 10 µm² aperture and 5 µm steps.

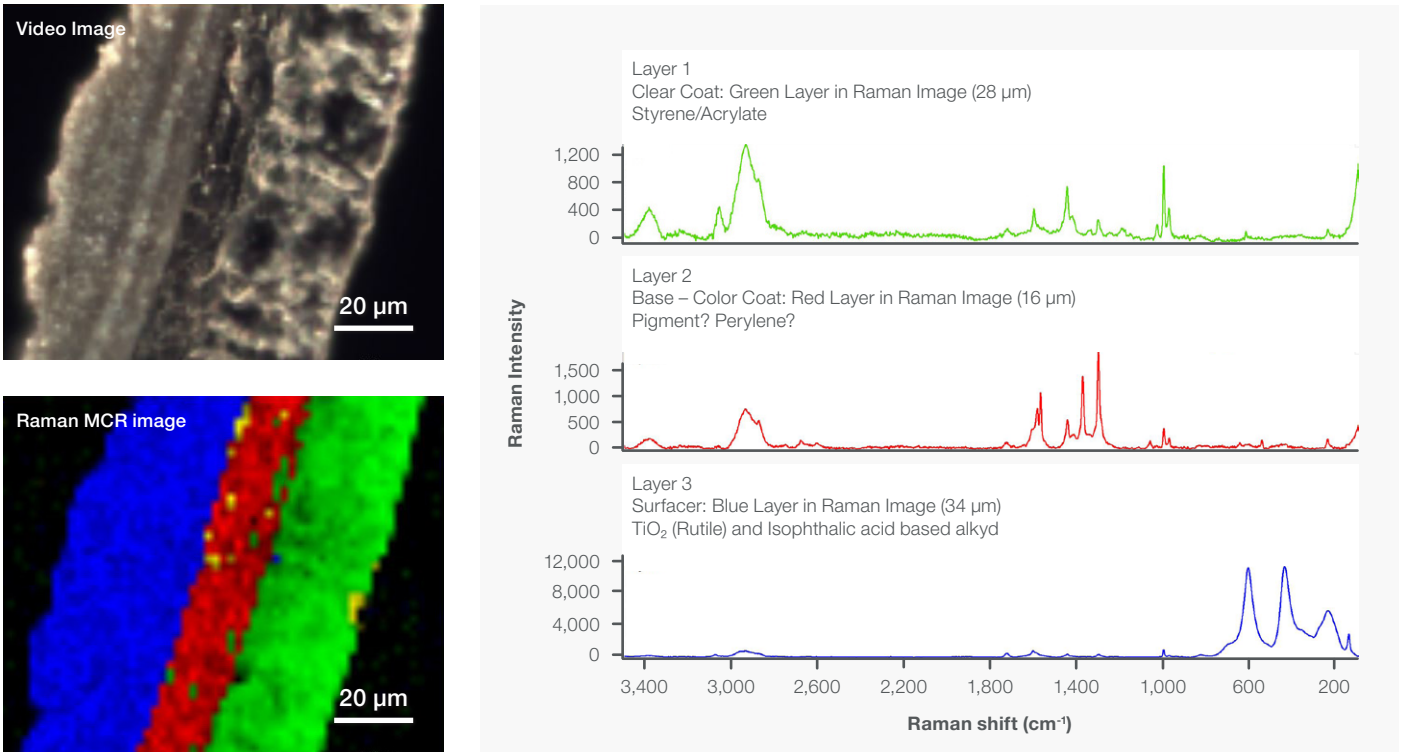

Figure 5. Representative Raman spectra from the first three layers of the door paint-chip sample (right). The fourth (epoxy) layer was lost during sample preparation. The spectra have been baseline corrected to remove fluorescence contributions and were collected using a 455 nm laser. An area 116 x 100 µm² was imaged using a pixel size of 2 µm. Video mosaic image of the cross-section (top left). Raman multivariate curve resolution (MCR) image of the cross-section (bottom left).

Raman paint chip analysis – automobile door

Figure 5 shows the Raman imaging analysis of the door paint-chip cross-section; this sample did not have the epoxy layer attached, as it was lost during sample preparation. However, since the Raman analysis of the epoxy layer was already determined to be problematic, this was not considered to be an issue.

The presence of styrene was much more prevalent in the Raman spectra from Layer 1 while the carbonyl peaks were much less intense compared to the infrared spectra.

There was a much more dramatic difference in the spectra from the first and second layers in the Raman analysis compared to FTIR. The best Raman match to the base-color coat was perylene; while it not an exact match, derivatives of perylene are known to be used for pigments in automobile paint, so it could represent the pigment in the color layer. The spectra from the surfacer layer were consistent with an isophthalic acid base alkyd, but also showed the presence of titanium dioxide (TiO_2, rutile), which can be difficult to observe with FTIR, depending on the spectral cutoff.

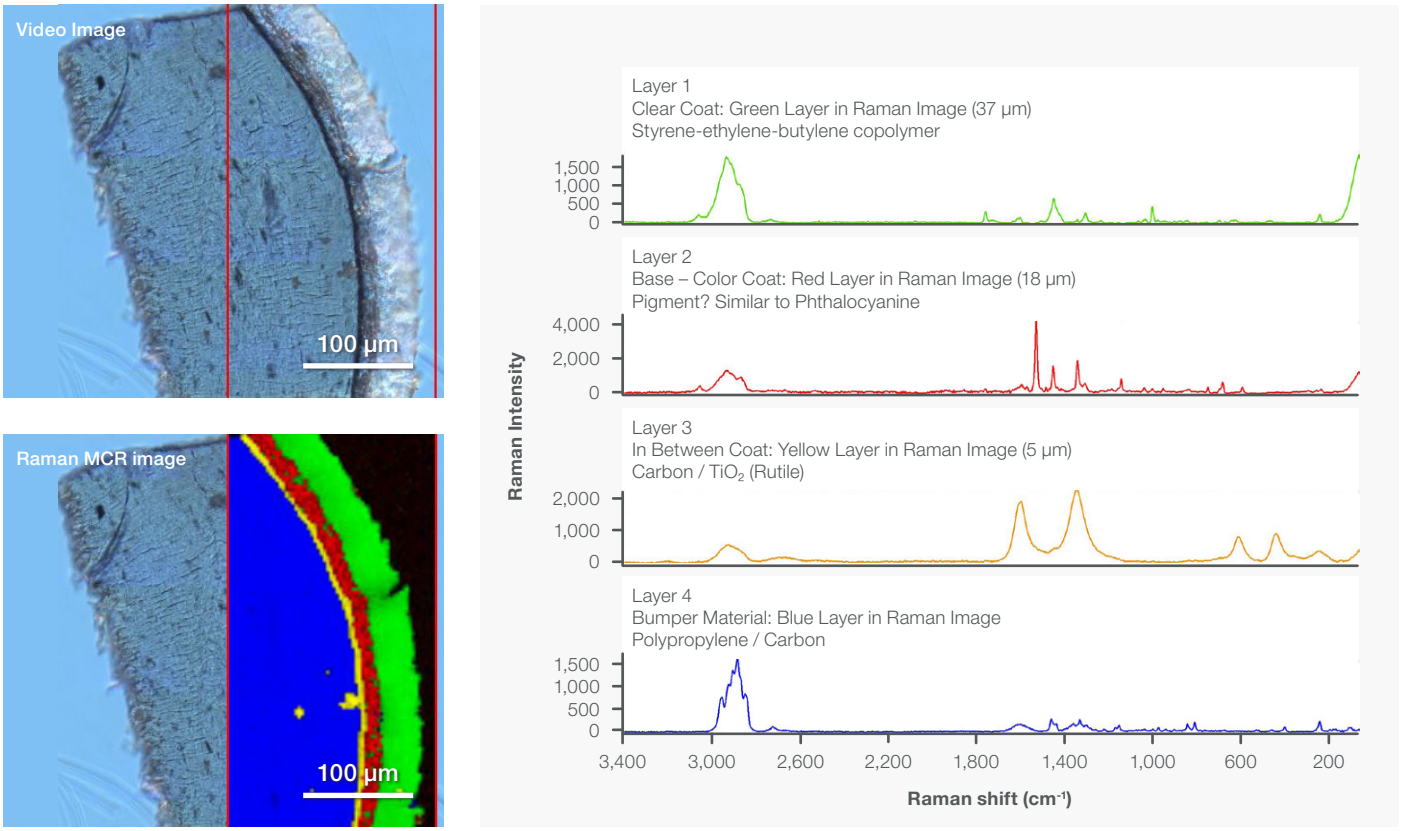

Figure 6. Representative Raman spectra from the bumper paint-chip sample (right). The spectra have been baseline corrected to remove fluorescence contributions and were collected using a 532 nm laser. An area 195 x 420 µm² was imaged using a pixel size of 3 µm. Video mosaic image of the cross-section (top left). Raman MCR image of a portion of the cross-section (bottom left).

Raman paint chip analysis - bumper

Figure 6 shows the Raman results for the bumper paint-chip cross-section. An additional layer (Layer 3) was observed, which was not detected with FTIR. The best match for the outer layer was a styrene-ethylene-butadiene copolymer, but there was also a small carbonyl peak that could not be accounted for, indicating an additional unidentified component. The spectrum from the base-color coat likely represents a pigment component because the spectrum matched, to some extent, phthalocyanine compounds that are used as pigments. The previously undetected layer is quite thin (5 µm) and contains carbon and rutile. Due to the thickness of the layer, and the fact that TiO_2 and carbon are more difficult to detect with FTIR, it is unsurprising that it was not captured by the infrared analysis. Consistent with the FTIR results, the fourth layer (bumper material) was identified as polypropylene, but Raman analysis also showed some carbon. While the presence of the talc seen with FITR cannot be ruled out, exact identification was not possible as the corresponding Raman peaks were too small.

Conclusions

Automobile paints are complex mixtures of components, and while this represents a wealth of identifying information, it also complicates their analysis. Paint chip evidence can be effectively probed using a Nicolet RaptIR FTIR Microscope. FTIR is a non-destructive analytical technique that delivers valuable information about the various layers and components in automobile paints. This application note focused on spectral analysis of paint chip layers, but further analysis of the results, either by direct comparison with a suspected automobile or dedicated spectral database, could provide additional information to match the evidence with its source.

Raman analysis with the DXR3xi Raman Imaging Microscope provided additional information on the paint chip samples. While FTIR and Raman are both vibrational spectroscopy techniques, this application note highlights how they can be used to identify different components of paints. Together, these techniques provide a more complete and complementary view of the samples. The extent of information that these techniques deliver from individual paint layers makes them valuable resources for the challenging task of forensic paint analysis.

Learn more at **thermofisher.com/forensics**

For research use only. Not for use in diagnostic procedures. For current certifications, visit thermofisher.com/certifications
© 2022 Thermo Fisher Scientific Inc. All rights reserved. All trademarks are the property of Thermo Fisher Scientific and its subsidiaries unless otherwise specified. AN53652_E 10/22M

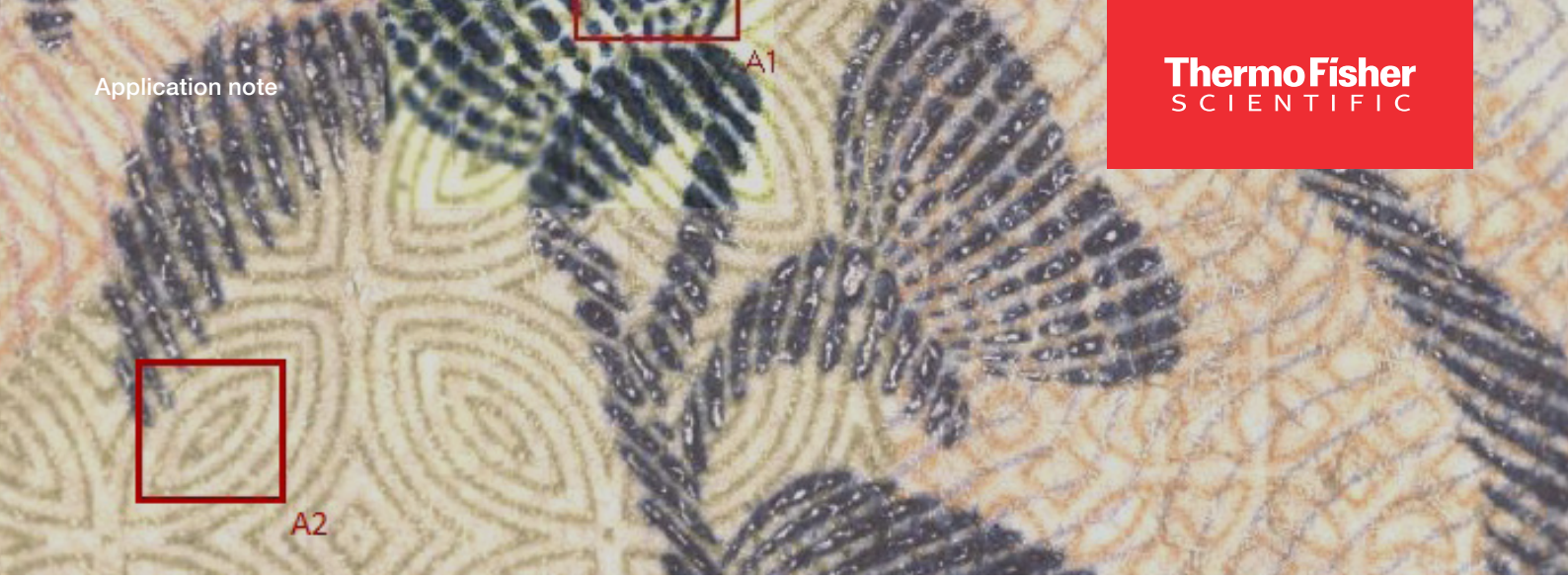

Application note

Analyzing inks and toners with FTIR microscopy

Forensic document analysis

The examination and authentication of documents is a typical focus of forensic science, and investigators are routinely asked to determine the origin and make up of a variety of written and printed materials, including letters, wills, contracts, checks, bank notes, seals, stamps, etc. This analysis looks at both the inks/toners as well as the paper onto which they are applied.

While most paper is primarily composed of cellulose, it can be processed in different ways and can contain a variety of additives and coatings. Ink analysis can require the differentiation of ink types, identification of ink sources, determining the sequence that inks were applied, or even ascertaining the age of the ink.



Figure 1. Nicolet RaptIR FTIR Microscope with ATR accessory.

FTIR microscopy

While a variety of analytical techniques are used for forensic document analysis, Fourier-transform infrared (FTIR) spectroscopy is typically utilized as an initial screening tool because it is non-destructive, and samples are conserved for any subsequent analyses. FTIR microscopy combines infrared spectroscopy and visible microscopy for joint visualization and chemical analysis of microscopic samples. FTIR microscopy can be used for single spot analysis, or it can create infrared images that use molecular information to show the spatial distributions of components across a sample area.

In this application note, a Thermo Scientific™ Nicolet™ RaptIR™ FTIR Microscope (Figure 1) was used to collect visual images and infrared data from a variety of ink and toner samples. The Nicolet RaptIR FTIR Microscope utilizes a motorized nosepiece to smoothly switch between a 10x visual objective and a proprietary 15x infrared objective. This allows you to quickly collect high-quality visual mosaic images and efficiently locate small samples or areas of interest. Switching to the 15x infrared objective provides you with higher-magnification visual images as well as optimized infrared spectra.

The infrared spectra in this application note were collected using a slide-on germanium-tip attenuated total reflectance (ATR) accessory on the 15x infrared objective. No additional sample preparation is needed for ATR data collection; the only requirement is contact between the ATR crystal and the sample. A pressure sensor in the microscope can automate sample contact using a customized contact pressure.

Complete forensic analysis of documents is an extensive topic beyond the scope of this application note. Instead, we will focus on obtaining spectra from a few types of inks/toners and discuss the factors that impact their analysis. An example where FTIR is used to differentiate between two overlapping types of blue ballpoint pen ink will also be presented.

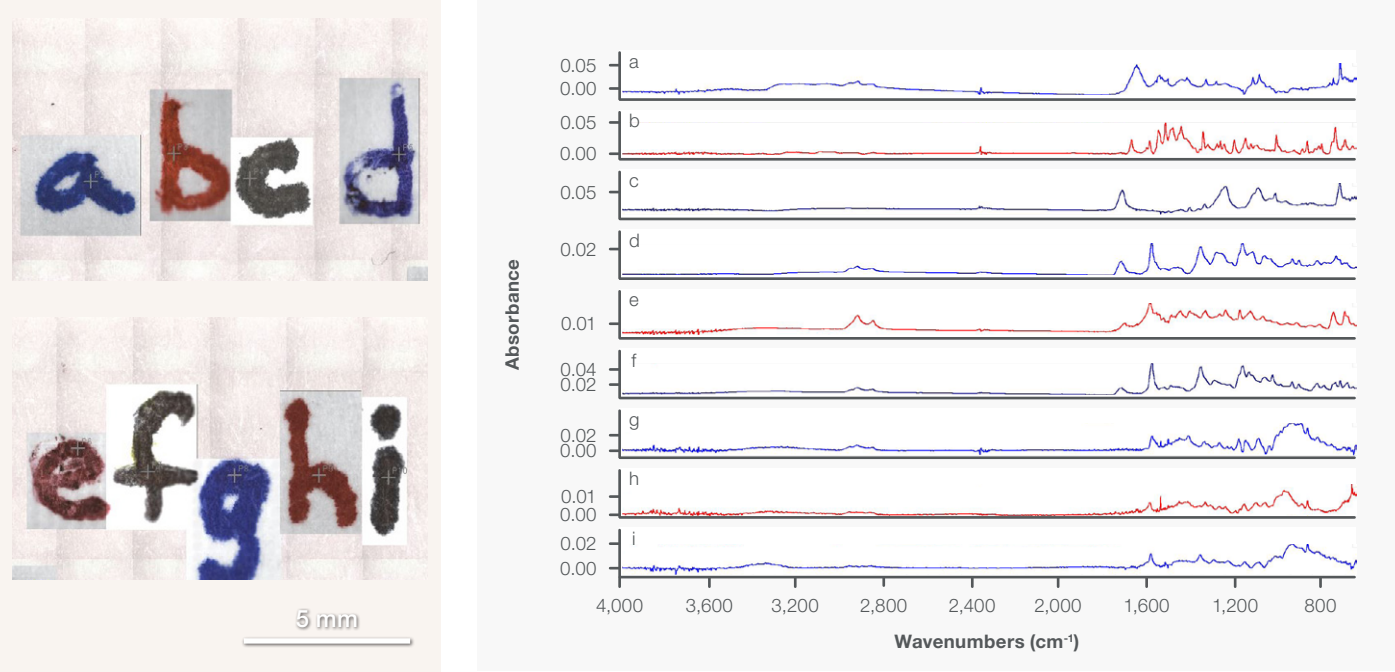

Figure 2. ATR infrared spectra from letters (a–i) handwritten on white paper with pens of assorted colors from various manufacturers. The paper spectrum has been subtracted to remove its contributions from the signal.

Ink analysis with ATR and FTIR

Spectra from various pens are shown in Figure 2. Initial measured spectra represent a mixture of contributions from the paper as well as the ink. Since each can consist of multiple components, it is usually advisable to sample from several points to evaluate potential variations in the spectral contributions of both the paper and the ink. The infrared contributions of the paper have been subtracted from each of the spectra shown in Figure 2.

Visual inspection of the spectra reveals clear differences between inks of different colors, and even between inks of the same color. There are also some cases where the inks are very similar, and differences are hard to evaluate just from visual inspection.

Ink analysis is not limited to handwritten samples. Figure 3 shows infrared images from two areas of a printed banknote. Data collected at the flower is based on a peak of calcium carbonate that is present in the ink. While paper can also contain calcium carbonate, the spatial evidence seems to indicate that this signal is primarily associated with the ink and not the paper. The second imaged area shows some of the background pattern; the infrared image is based on a carbonyl peak of an ink component. While it was possible to differentiate the ink from the paper, the ink signal was much weaker for the background pattern than the flower. This is likely because the ink used in the flower is raised and sits on the paper surface, whereas the background pattern appears to penetrate the paper more significantly. This illustrates a critical consideration for this kind of analysis: ATR is a surface technique, and the less ink that is present at the surface, the weaker the signal will be. This makes it much more complicated to deconvolute the contributions of the ink from the paper.

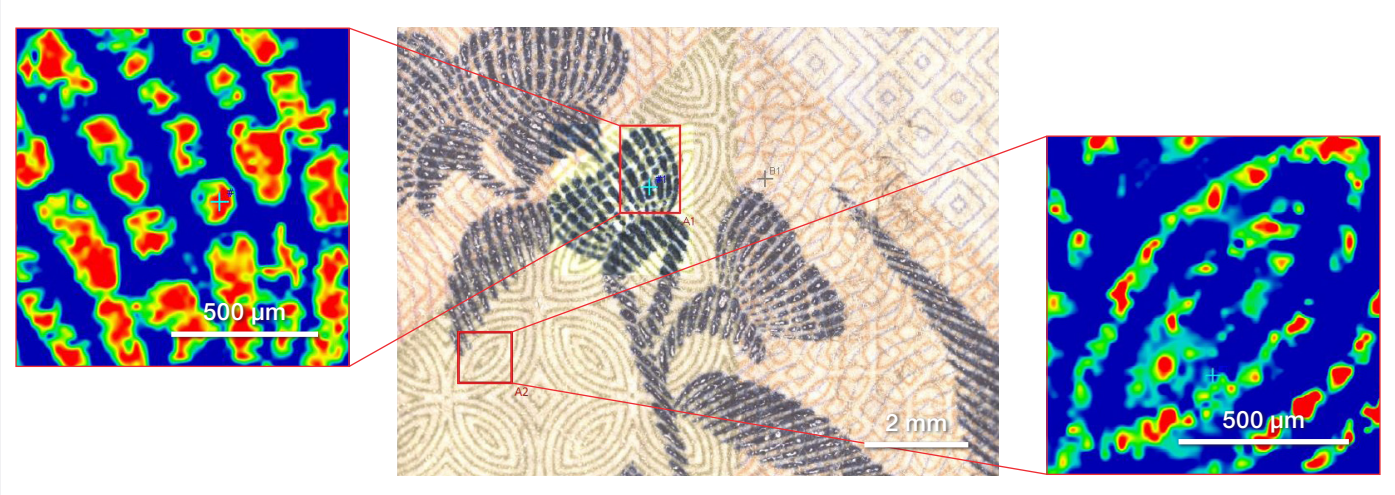

Figure 3. Infrared images generated from the printed designs on a banknote. Peak area images were generated for the flower, using a calcium carbonate peak at 871 cm^{-1} (left), and the background pattern, using a carbonyl peak at 1735 cm^{-1} (right).

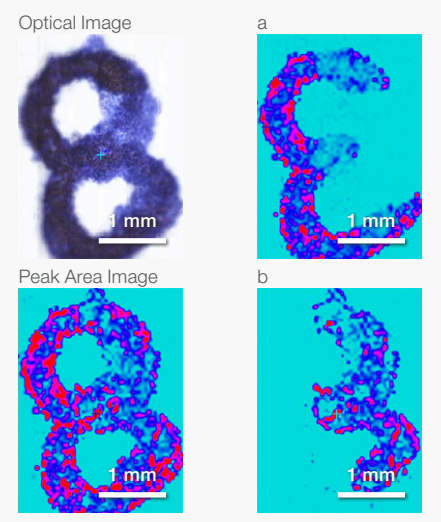

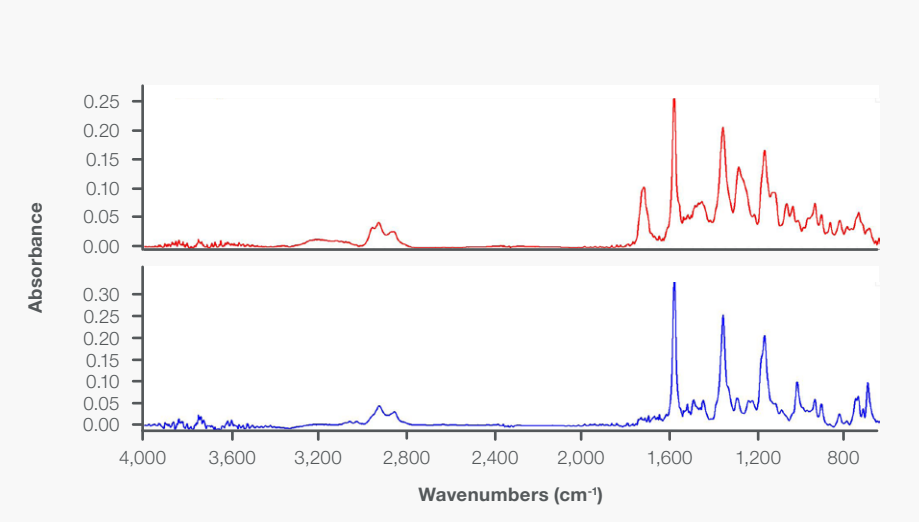

Figure 4. Infrared ATR images of two different inks used to write the number "8". a) The original "3" can be seen in the infrared image based on the peak at 1722 cm^{-1}. b) Infrared image of the second ink that was used to change the "3" into an "8," based on the peak at 701 cm^{-1}. The paper spectrum has been subtracted to remove its contributions from the signal.

Deconvoluting mixtures of inks

Figure 4 shows the differentiation of two blue inks used in a handwritten number. Microscopic visual inspection of the "8" shows some inconsistencies in the ink, but additional confirmation would be critical for any enforcement action. Infrared analysis of the ink shows that the "8" is clearly made up of two distinct types of blue ink, and that the "3" was modified to make it look like an "8." Both ink spectra have peaks that are consistent with a blue pigment (Victoria blue/methyl blue), but the ink of the "3" appears to contain an additional alkyd resin not found in the other ink. This demonstrates how FTIR can be used to differentiate between two inks without the need for a full database and discriminate methods.

Toner analysis with FTIR

Rather than printing with ink, laser printers utilize toner, which is a powder-based medium. Figure 5 shows infrared spectra from several colored lines generated on a laser printer, which uses a microscopic mixture of 4 toners (black, cyan, magenta, and yellow) to generate printed colors. Toners typically have a polymer base with added pigments; this polymer resin base generally dominates the infrared spectra due to its high proportion relative to the pigment.

In Figure 5, the infrared spectra for all toners appear to be largely the same, save for some minor differences. For example, the spectra from the red, green, and yellow lines appear to be discreet from the black and blue lines; this is likely the result of all three colors utilizing yellow toner. Some of the smaller peaks can therefore be attributed to the yellow pigment. Overall, it appears that differences in the resin base would be easier to distinguish due to the minor signal contribution from the pigments. This means that documents from different laser printers will likely be more difficult to tell apart unless there are distinguishing features in their respective resin bases.

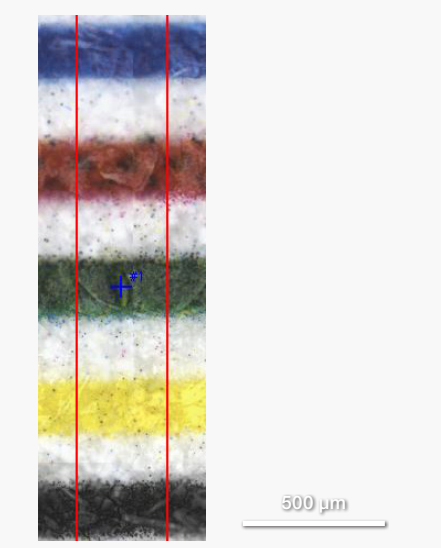

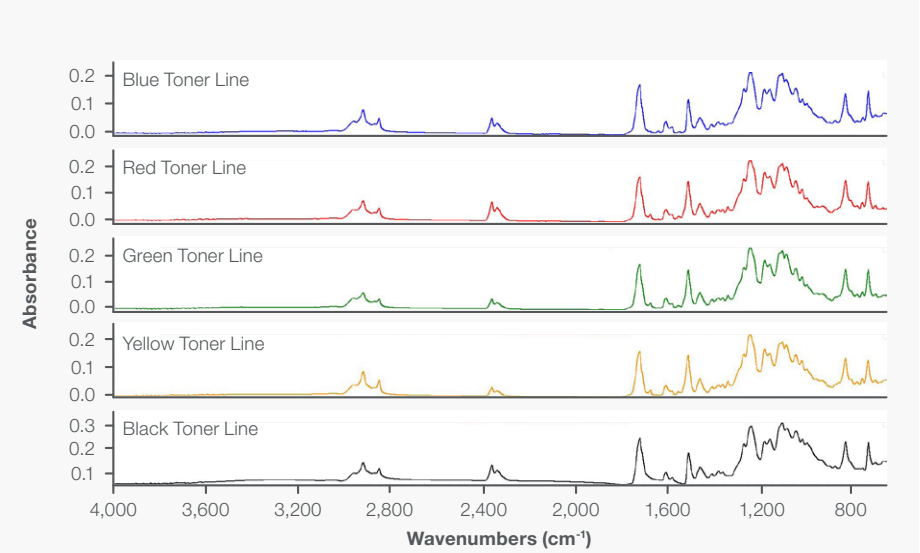

Figure 5. ATR infrared spectra from lines printed using a laser printer. The colored lines are made up from a mixture of up to four toners (black, yellow, cyan, and magenta).

Conclusions

The Nicolet RaptIR FTIR Microscope provides exceptional visual and spectroscopic insights into ink and toner samples. The non-destructive FTIR analysis preserves evidence for further testing, or presentation in court, while providing specific and detailed information about the sample. As shown, even in cases where a document was altered, the spectral data can be used to differentiate between inks. The speed and specificity combine to make the Nicolet RaptIR FTIR Microscope an ideal tool for any forensics laboratory.

Learn more at **thermofisher.com/forensics**

For research use only. Not for use in diagnostic procedures. For current certifications, visit thermofisher.com/certifications
© 2022 Thermo Fisher Scientific Inc. All rights reserved. All trademarks are the property of Thermo Fisher Scientific and its subsidiaries unless otherwise specified. AN53650_E 10/22M

Application note



Forensic analysis of fiber and hair using FTIR microscopy

Introduction

Fibers and hairs are abundant and easily transferred trace evidence that can link individuals or items to a crime scene or contact with a victim. Textiles represent a major source of fibers and are either of natural origin or manmade synthetics. Light microscopy, including the use of polarized light, is commonly used for fiber analysis, and an experienced analyst can categorize fibers based on their physical appearance and perform a direct comparison with fibers from known sources. The success and reliability of this analysis, unfortunately, largely depends on the experience of the analyst. Fourier-transform infrared (FTIR) microscopy provides supporting information for fiber analysis while also being less dependent on user experience. Spectra obtained from FTIR microscopy can be used to quickly identify fiber materials. It is also possible to do a direct comparison between fibers to help verify a suspected source. As FTIR microscopy is a non-destructive technique, it can be followed by other, potentially destructive, analytical methods for further characterization and verification.

Hair is primarily composed of protein, but other components may also be present in smaller quantities, including water, lipids, dyes, cosmetic residues, etc. Infrared spectra of hairs are generally quite similar, but differences caused by chemical treatments (bleaching, straightening, etc.) and/or sun exposure that affects the cuticle (outer protective layer) of the hair can be detected. Infrared spectra of hair can also show differences based on race, gender, age, diet, and health. Classifying an unknown hair sample to this degree, based only on its spectrum, would require chemometric methods and large databases comprised of representative spectra. FTIR microscopy is, therefore, better suited for providing corroborating information on hair samples as it is quick, easy, and non-destructive, allowing it to serve as the first step in an analysis workflow. Direct comparison of spectra from an unknown hair sample to a limited number of known sources is much more manageable.

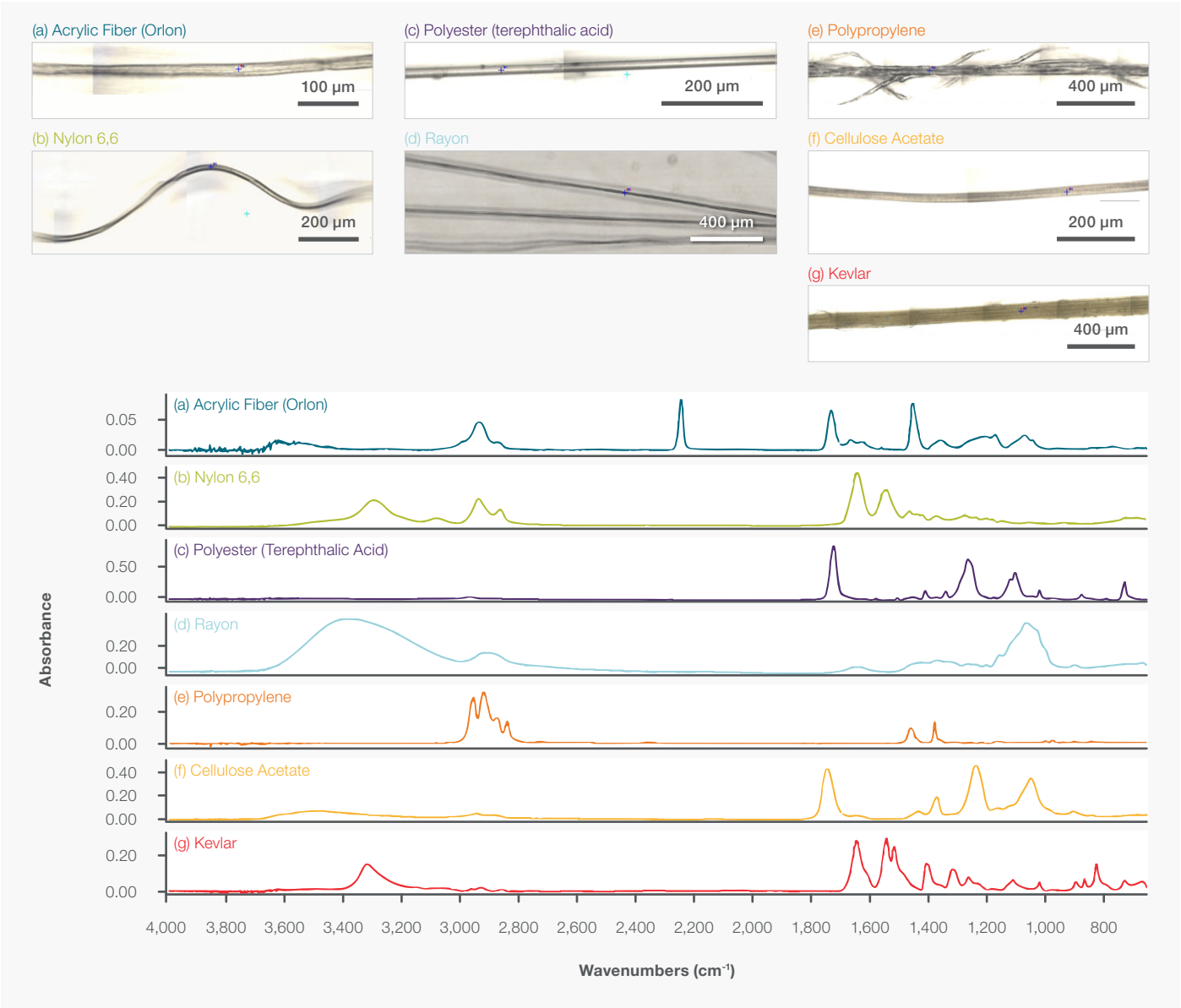

Figure 1. Infrared spectra from a selection of synthetic fibers. Video mosaic images were collected using the 15x objective; spectra were collected using a slide-on germanium ATR accessory.

Experimental details

A Thermo Scientific™ Nicolet™ RaptIR™ FTIR Microscope was used to analyze the fiber and hair samples in this application note. The Nicolet RaptIR FTIR Microscope easily locates regions of interest with a 4x visible objective lens, which is used to quickly collect a large, high-quality visual mosaic. The microscope then automatically switches to a proprietary 15x objective for both excellent higher magnification visual images as well as infrared spectra. A germanium slide-on attenuated total reflection (ATR) accessory allows for the collection of spectra with little to no sample preparation. A built-in pressure sensor can be used to adjust the automatic contact between the sample and the ATR crystal, ensuring the pressure is both repeatable and customizable for different samples. For most of the fiber and hair specimens, several positions along the sample were selected for automatic spectra collection in order to verify homogeneity. The high-precision stage ensures that spectra are collected from the positions chosen in the visual mosaics. For infrared mapping, an area and step size are selected, and ATR spectra are then automatically collected over that area.

Synthetic fibers

A selection of 7 synthetic fibers was analyzed, with visual images and FTIR spectra shown in Figure 1. The differences in the infrared spectra make it relatively straightforward to use commercial libraries for fiber material identification. Distinguishing between different fibers of the same material, meanwhile, is largely sample dependent; for instance, contributions from dyes and other additives might prove to be unique to a particular source. These are, however, relatively minor components, and a direct comparison between an unknown fiber and fibers from possible matching sources will likely prove to be more definitive.

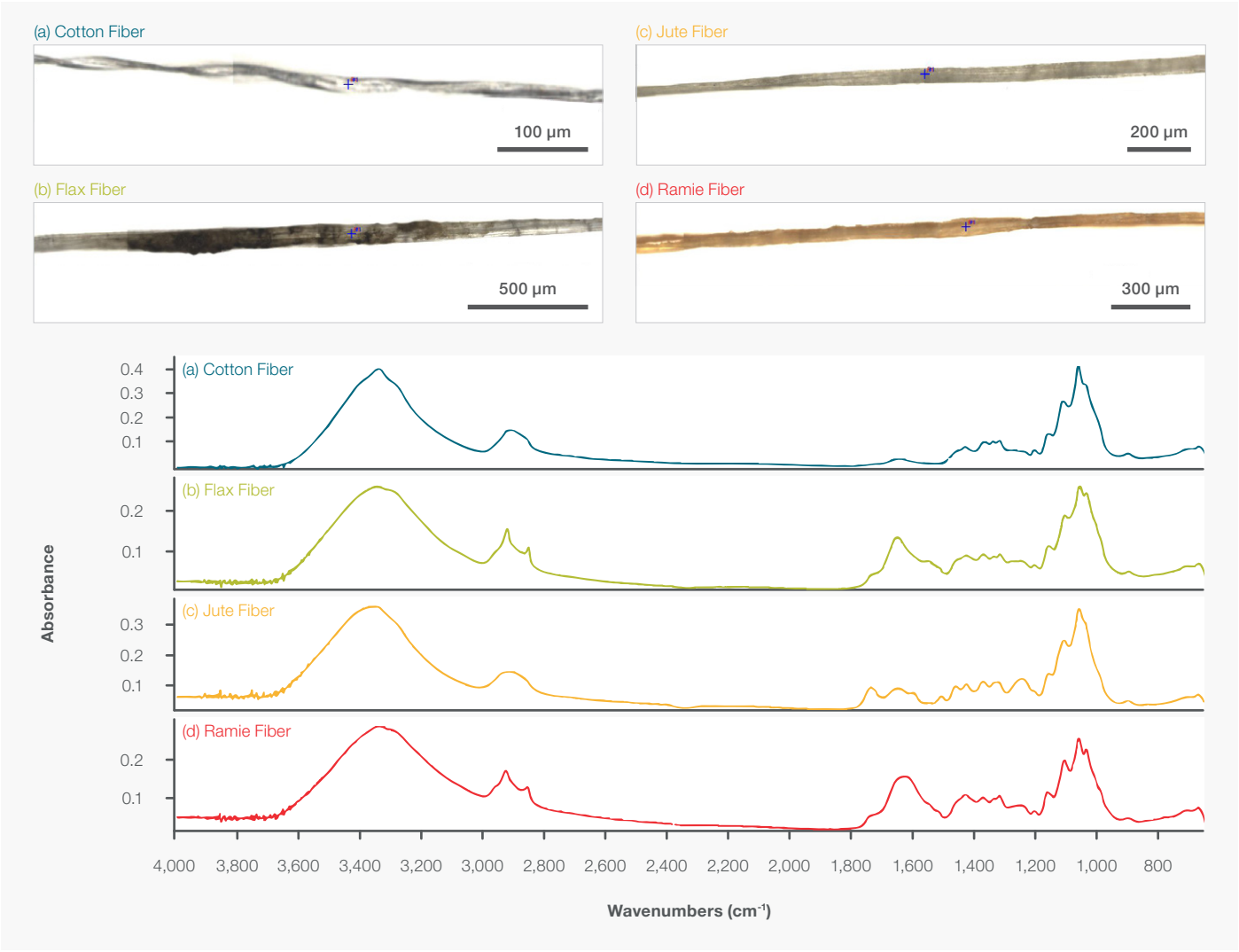

Figure 2. Infrared spectra from cellulose-based fibers. Video mosaic images were collected using the 15x objective; spectra were collected using a slide-on germanium ATR accessory.

Natural fibers

Similar to their synthetic counterparts, natural fibers can readily be categorized based on their general material (cotton, keratin, etc.). However, differences within a class of material are more subtle. Figure 2 shows the analysis of four different cellulose fibers; cotton, flax, jute, and ramie. Their infrared spectra are largely similar but can be differentiated. Within a particular type of cellulose fiber, differences associated with dyes and processing treatments are still best suited for a direct comparison of an unknown fiber to fibers from known sources.

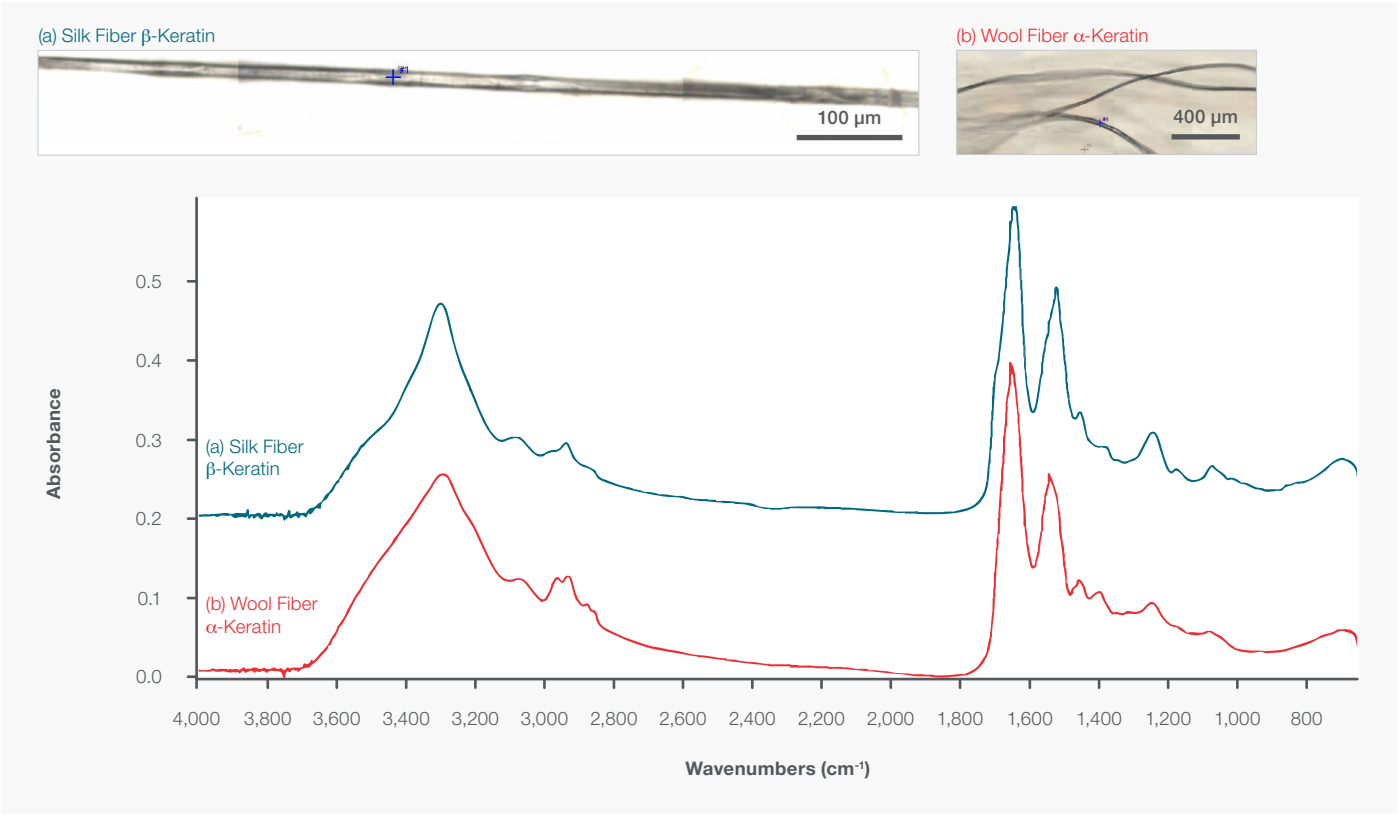

Figure 3. Infrared spectra from keratin-based textile fibers. a) Silk, composed of β-keratin. b) Wool, composed of α-keratin. Video mosaic images were collected using the 15x objective; spectra were collected using a slide-on germanium ATR accessory.

Another distinct group of natural fibers are those made of keratin and other fibrous proteins. This includes wool and silk fibers, which are commonly used in textiles. Wool, like human hair, is mainly α-keratin, whereas silk is composed of β-keratin; a comparison of their infrared spectra can be seen in Figure 3. Since these materials are chemically similar, so are their infrared spectra; nevertheless, there are still enough differences to distinguish between them.

Embedded fibers

Fibers do not always appear as loose strands; they can also be part of a larger sample. Figure 4 shows an example of a nylon fiber embedded in a paper substrate. Since ATR is a surface analysis technique, the fiber can only be observed when it is above the surface of the paper, as is seen in Figure 4. This example shows peaks for both a synthetic fiber and a matrix of natural origin (paper cellulose).

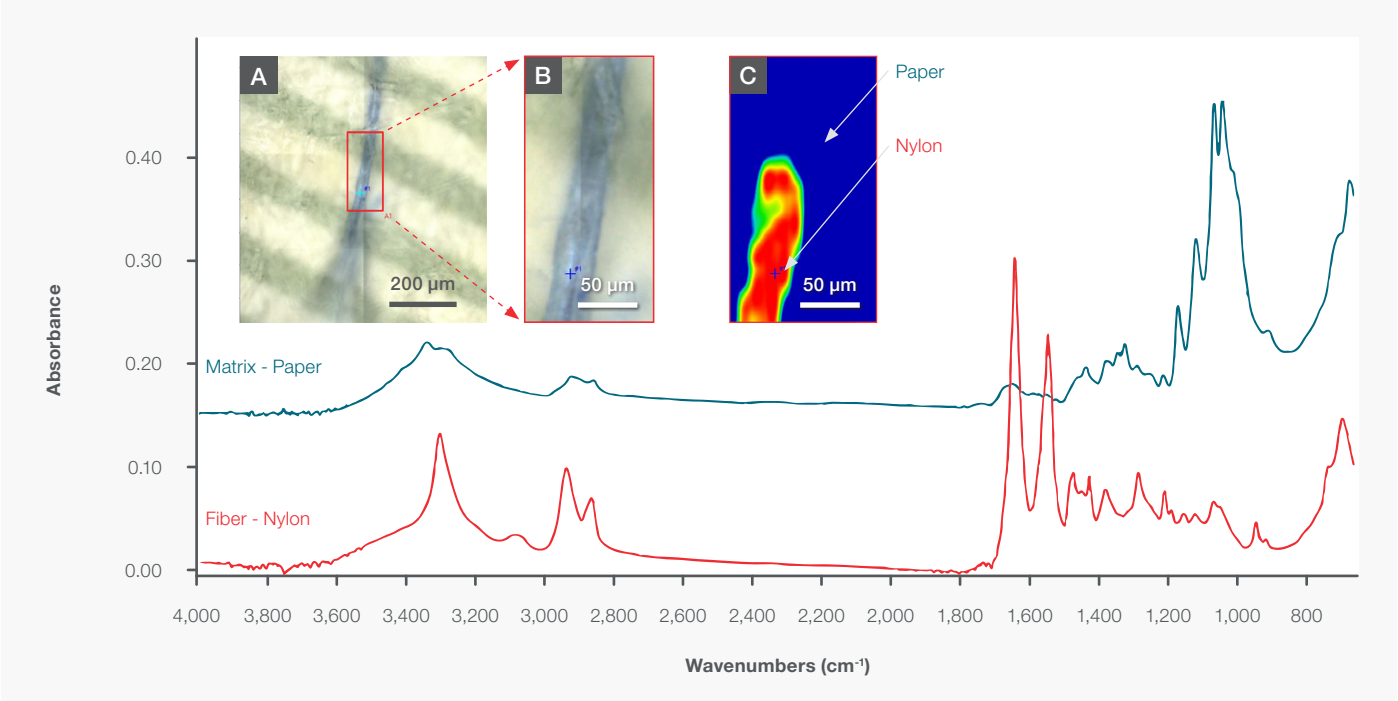

Figure 4. Infrared ATR mapping of a nylon fiber embedded in a paper substrate. a) Video mosaic collected using the 15x objective. b) Video image of the sample area being analyzed. c) Infrared correlation image based on the nylon spectrum from the sample. Area: 110 x 240 µm², effective aperture: 25 x 25 µm², 10 µm steps, 300 spectra total.

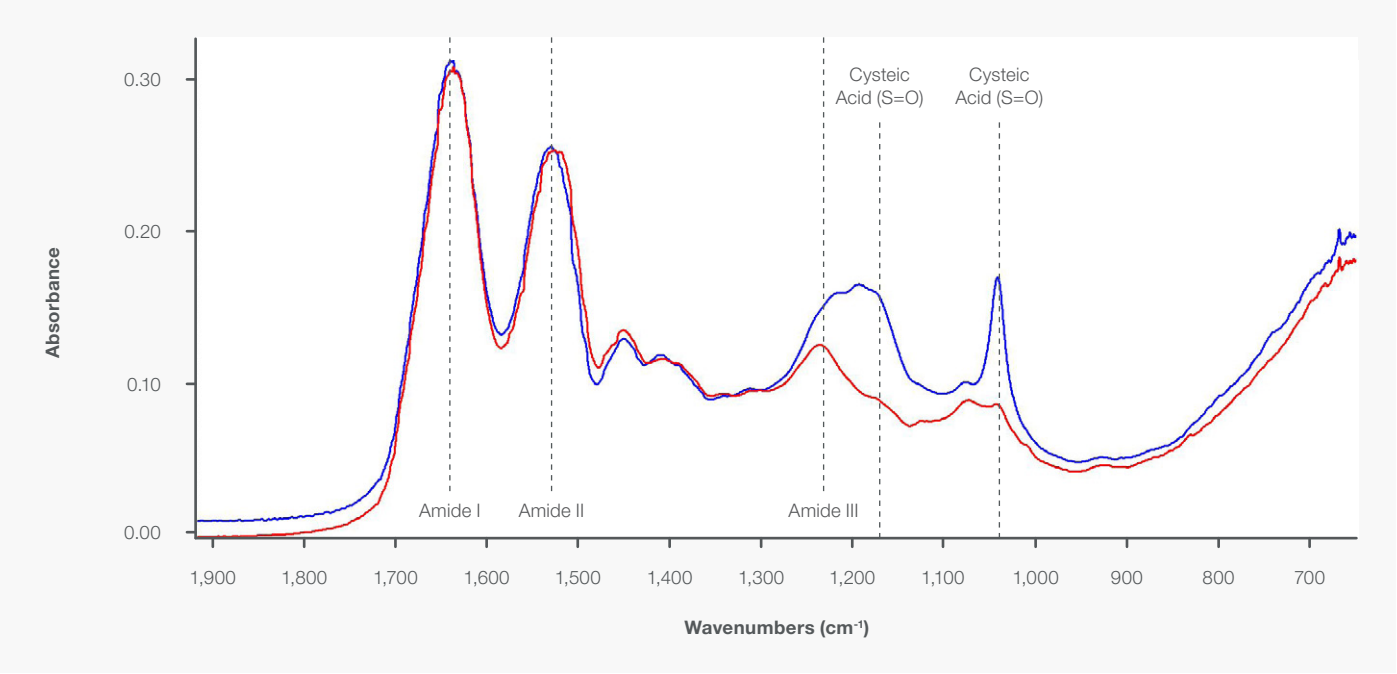

Figure 5. Infrared spectra from an untreated hair sample (red) and a treated hair sample (blue). Stronger peaks associated with cysteic acid are observed in the treated hair sample.

Hair

Like wool, hair is made of α-keratin, however, hair fibers are typically linked to particular people/pets rather than textile sources. While the basic chemical structure of all hair is very much the same, differences can arise from chemical treatments such as bleaching, straighteners, and dyeing. One common effect is the oxidation of sulfur during hair treatments, resulting in the disruption of disulfide bonds in hair. Oxidation of cystines can produce cysteic acid with an enhanced peak at 1042 cm^{-1}. There is also an additional cysteic acid peak at ~1077 cm^{-1} that is often observed as a shoulder on the amide III peak. A comparison of untreated and treated hair can be seen in Figure 5, illustrating the effect that chemical treatments can have on the structure of hair and the corresponding infrared spectra.

Distinguishing hair from different sources can be challenging but is simplified when direct comparisons can be made between unknown and known hair samples. Figure 6 shows such a comparison, with samples from three different individuals living in the same dwelling. A spectrum of cat hair was also included for comparison. While the basic structures are the same, there are still differences in the spectra that could be used to distinguish them.

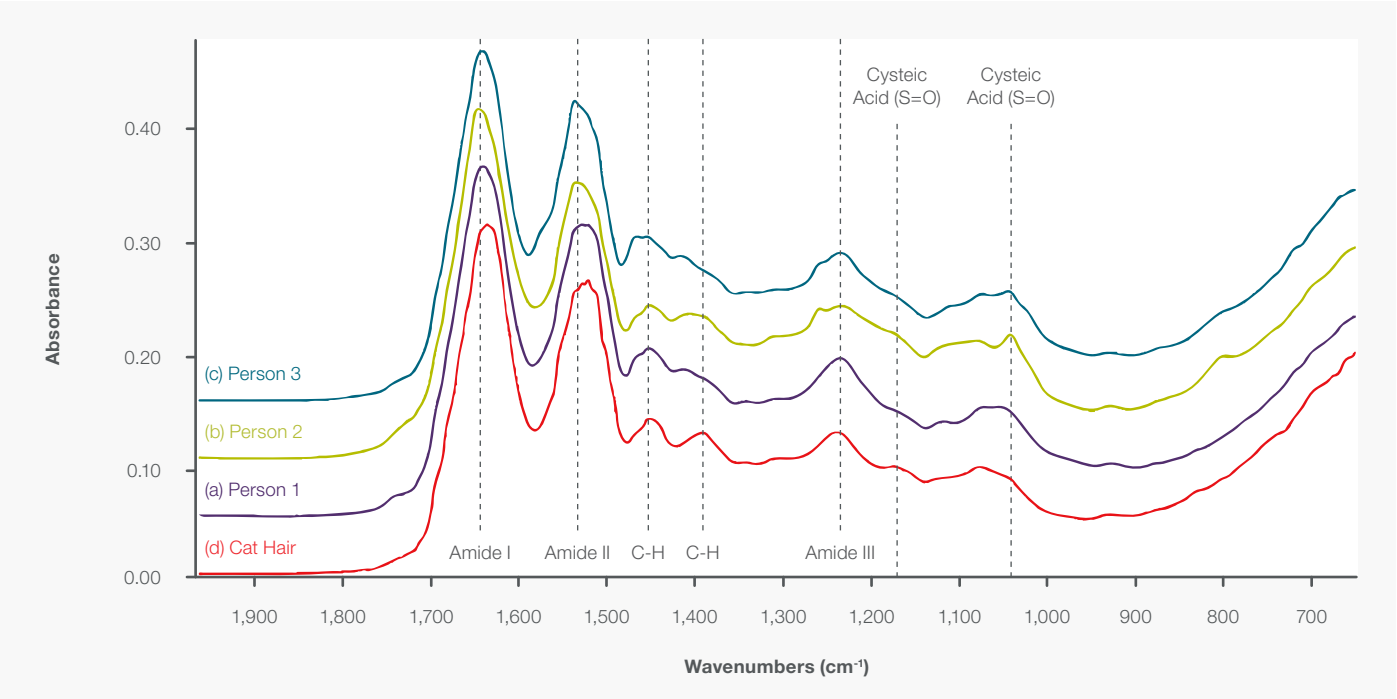

Figure 6. Infrared spectra from three individuals, (a) a male adult, (b) a female child, and (c) a female adult, living in the same dwelling, as well as (d) cat hair. Differences include shifts in the amide I and amide II bands, the C-H bending regions, and the area associate with cysteic acid.

In these situations, it is possible to generate a discriminant analysis method where spectra from multiple sources serve as the basis for classification; it could then be determined which class an unknown sample belongs to. In this application note, the discriminant analysis method was generated using Thermo Scientific™ TQ Analyst™ Software; the method was then validated using the hair spectra from the three individuals. In each case the spectra were classified correctly. This analysis can subsequently be used to determine if an unknown hair sample belongs to one of these known sources. To classify hairs based on general characteristics such as race, gender, and diet would require much more extensive and representative databases and more complex and carefully constructed chemometric methods. While some attempts have been made to achieve this, it is not clear if this is practical for such a wide-ranging classification because of the amount of data involved and all the possible variables that would need to be considered.

Conclusions

FTIR microscopy provides two tiers of fiber analysis. The first is a fast, easy, and effective compositional analysis for a particular fiber. This general classification is quite straightforward and can be effective with a minimal amount of experience. The use of ATR requires very little sample preparation, is non-destructive, and provides a wealth of information on the fibers' chemical structure. This initial classification can be used as the first step in an analysis workflow, directing subsequent tests.

The second tier of fiber analysis involves assessing variations within the same class of material. While this is much more sample dependent, the examples highlighted in this application note show that there can be sufficient differences between fibers of the same material that the spectrum of an unknown sample can be matched to fibers from known sources. Hair in particular can be analyzed in this fashion; hair treatments such as bleaching, dyeing, and straightening can show intense differences. While this type of analysis requires the collection of additional spectral information, it has the potential to link an unknown fiber to a specific source.

Learn more at **thermofisher.com/raptir**

For research use only. Not for use in diagnostic procedures. For current certifications, visit thermofisher.com/certifications
© 2023 Thermo Fisher Scientific Inc. All rights reserved. All trademarks are the property of Thermo Fisher Scientific and its subsidiaries unless otherwise specified. AN56360_E 01/23M

Application note



Analysis of a Tintoretto stratigraphy with micro-FTIR spectroscopy

Authors

Barbara Bravo (Thermo Fisher Scientific),
Francesca Caterina Izzo,
Elisabetta Zendri, Eleonora Balliana
(Ca' Foscari University of Venice)

Introduction

In this application note, a painting sample (stratigraphy) of Tintoretto's work at the Scuola Grande di San Rocco (Venice, Italy) was analyzed in order to verify the composition of its five pictorial layers. Specifically, the analysis sought to determine if:

- The top of layer (1) contained oil as a binder
- The intermediate layer (2) has tempera grassa (a mixture of protein and oil) as a binder, and what pigments it contains
- The greenish layer (3) is the result of mixing malachite and earth pigments
- The earth pigments in the ground/preparation layer (4) are mixed with biacca or cerussite, and if proteins are present as the main binder

Fourier transform infrared (FTIR) spectroscopy has long been utilized in art restoration to investigate stratigraphy structure, specifically to identify binders, pigments, and other materials used in the preparation layers. Thanks to the availability of spectral libraries, it is possible to easily identify all the spectra acquired.

Sample

The stratigraphy sample, kindly provided by Dr. Eleonora Balliana, was taken from the ceiling of the Scuola Grande di San Rocco in Venice (Figure 1). Ten years after the completion of the Sala dell'Albergo, between 1576 and 1577, Tintoretto completed the large canvases in the Sala Capitolare. The decorative cycle focuses on scenes from the Old and New Testament. The ceiling analyzed in this application note in particular shows three main moments of the Jewish people's journey to the Promised Land.



Figure 1. Sala Capitolare of the Scuola Grande di San Rocco in Venice.

The sample is a purple veil fragment collected from the glaze used to coat a depiction of a snake (Figure 2).

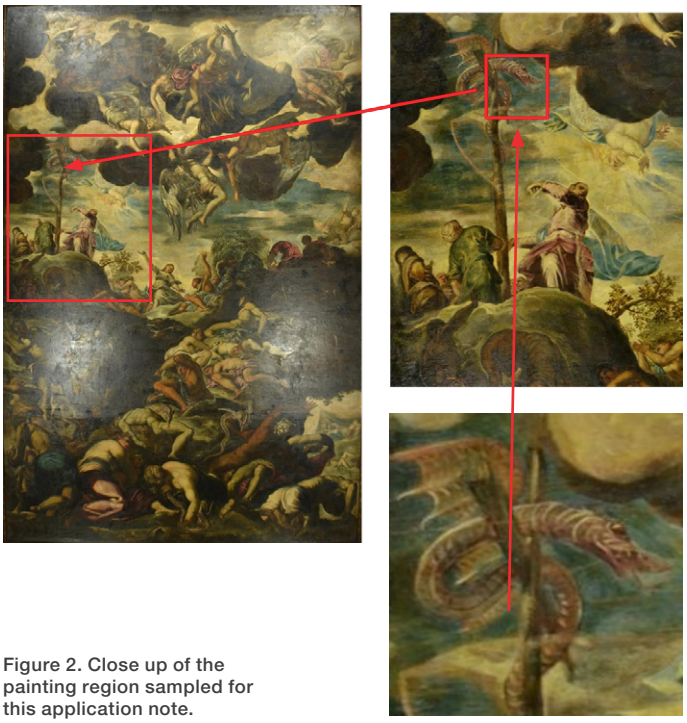

Figure 2. Close up of the painting region sampled for this application note.

Sample preparation

The painting sample was embedded in resin in order to obtain the stratigraphy along with visible, ultraviolet (UV), and scanning electron microscopy energy dispersive spectroscopy (SEM-EDS) images. The sample consists of four well-defined layers and a sketched fifth layer containing many small inclusions.

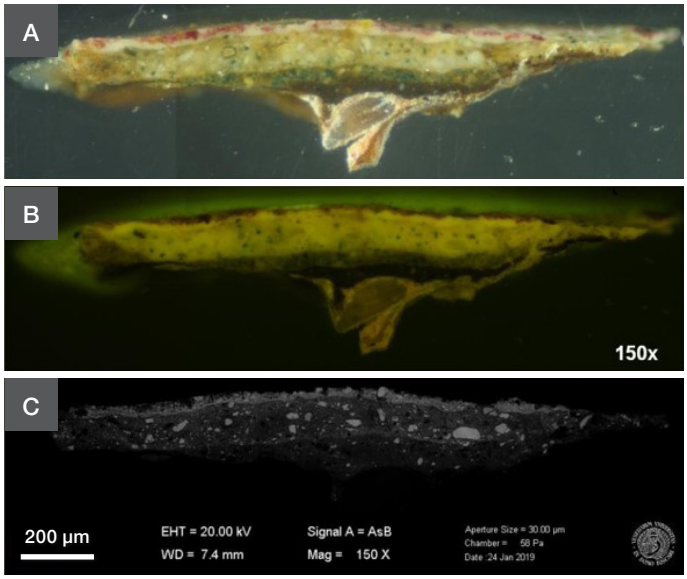

Figure 3. Cross section of the painting sample embedded in resin, shown with visible, UV, and SEM-EDS imaging (A to C).

This sample exemplifies Tintoretto's pictorial technique, where thin layers are applied on top of each other. The presence of a dark ground layer (4) is also typical for Tintoretto; it is used to create shadows and facilitate the application of the surrounding areas. Layers 2 and 3 are expected to consist of pictorial drafting of the snake's body, which was then detailed through the application of a purple glaze (1) mixed with other materials.

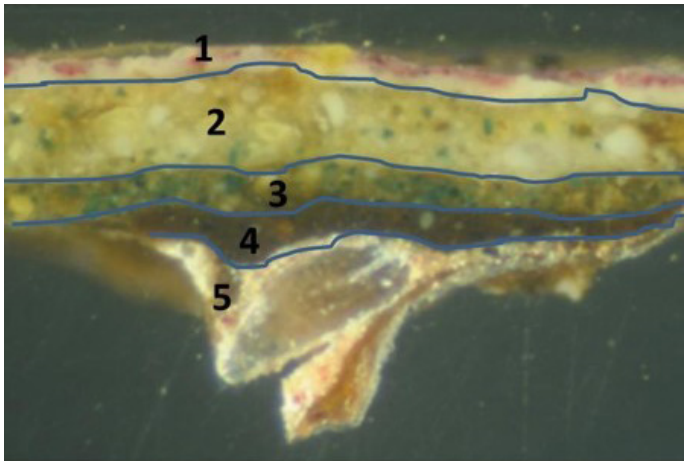

Figure 4. Close up of the painting sample showing its pictorial layers.

Analysis

The sample was analyzed using a Thermo Scientific™ Nicolet™ RaptIR™ FTIR Microscope, which offers precision and agility for streamlined sample analysis, producing rapid, actionable results. It can often be a lengthy and difficult process to pinpoint the intricacies of a sample and find the answer you need. Any amount of time savings can make a world of difference in delivering prompt, actionable results. The research-grade Nicolet RaptIR Microscope is not just suitable for users of all experience levels, but also for numerous disciplines. The objectives, infrared capability, and clear images are useful in a diverse range of fields including pharmaceuticals, environmental research, forensics, art restoration, as well as polymers and materials research.



Figure 5. The Thermo Scientific Nicolet RaptIR FTIR Microscope with a Nicolet iS50 FTIR Spectrometer.

Methods

First, a visual mosaic was collected using the 4x objective, followed by a visual and IR mosaic using the 15x objective. The resulting spectral resolution was 8 cm^{-1} with a 1 second acquisition time for each spectrum.

Multiple maps mode

Spectra were acquired in ATR mode using a germanium crystal with pressure control in order to avoid damaging the sample.

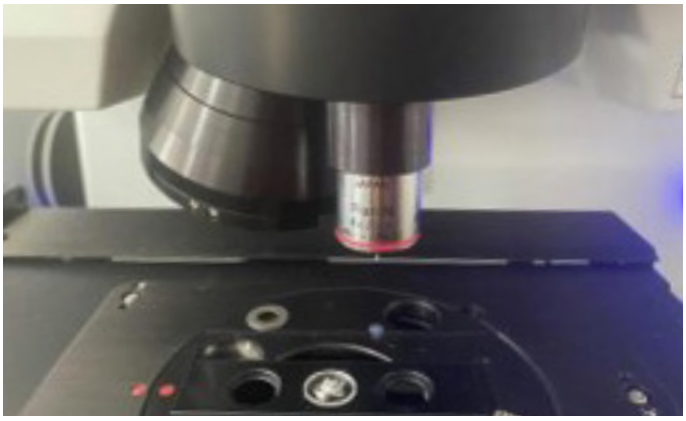

Figure 6. The 4x and 15x objectives of the Nicolet RaptIR FTIR Microscope.

Results

The 4x visual mosaic provided a picture of the regions within the stratigraphy; the subsequent 15x visual mosaic provided greater detail for each region of the sample.

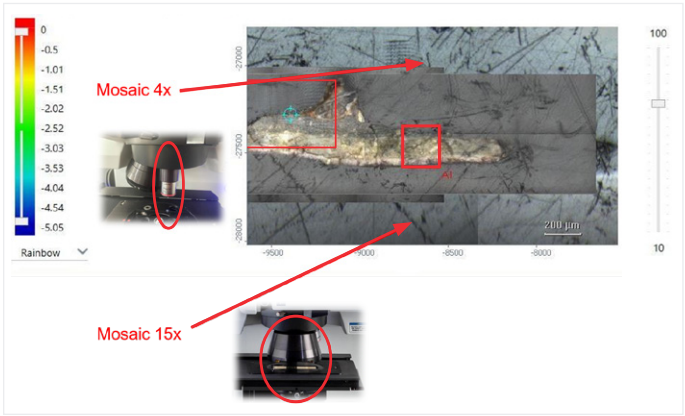

Figure 7. 4x and 15x maps and objectives.

Multiple maps were acquired in ATR mode to obtain more information from different regions of the sample (Figure 8).

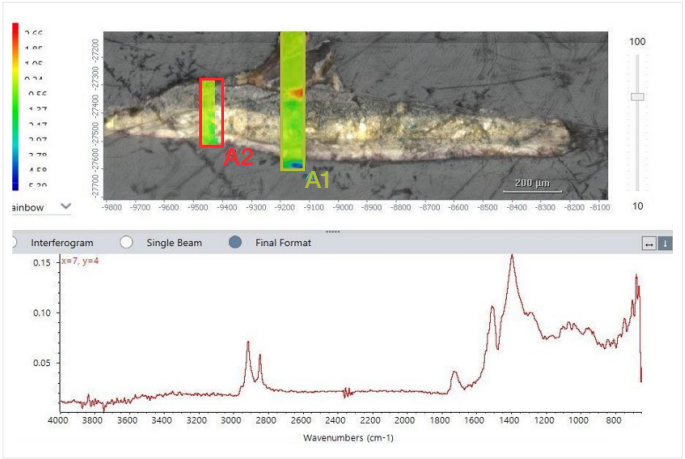

Figure 8. 15x mosaic, maps, and a real-time spectrum. An in-progress correlation with organic substances is boxed in red. A1 shows a map that has already been acquired, A2 shows the active acquisition. The corresponding spectrum is shown in real time.

Correlation maps were created using the correlation function of Thermo Scientific™ OMNIC™ Paradigm Software in order to evaluate the presence of the different materials.

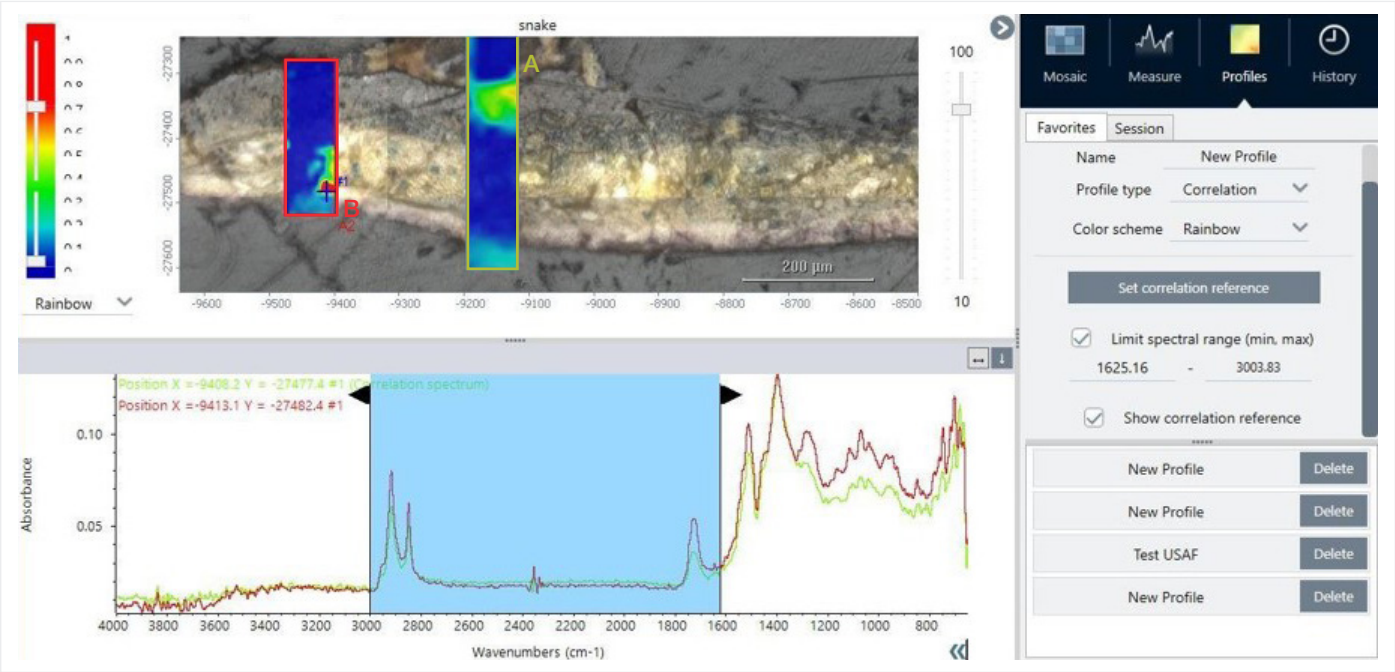

Figure 9. Oil correlation maps. Labels A and B indicate regions where oils are present. A corresponds to the upper pictorial film (1) and B corresponds to the preparation layer (4).

Oil correlation maps

Using OMNIC Paradigm Software, it is possible to correlate all the spectra acquired in the mosaic with the characteristic bands of natural oils, as seen in Figure 9. The results (marked A and B) indicated the presence of a lipidic binder, most likely linseed oil, which was detected not only in the upper pictorial film (1) but also in the preparation layer (4). There are also signals that are linked to the presence of proteins, silicate, etc. This was expected, as the use of oil and protein mixtures is typical for Tintoretto.

Protein correlation maps

The presence of protein (likely animal glue) was found in the ground/preparation layer, close to the canvas (Figure 10). Animal glue was commonly mixed with white lead or earth pigments by Tintoretto to create an ideal optical layer and drastically reduce the absorptivity of the canvas. Signals associated mainly with gypsum and lead carbonate are also visible.

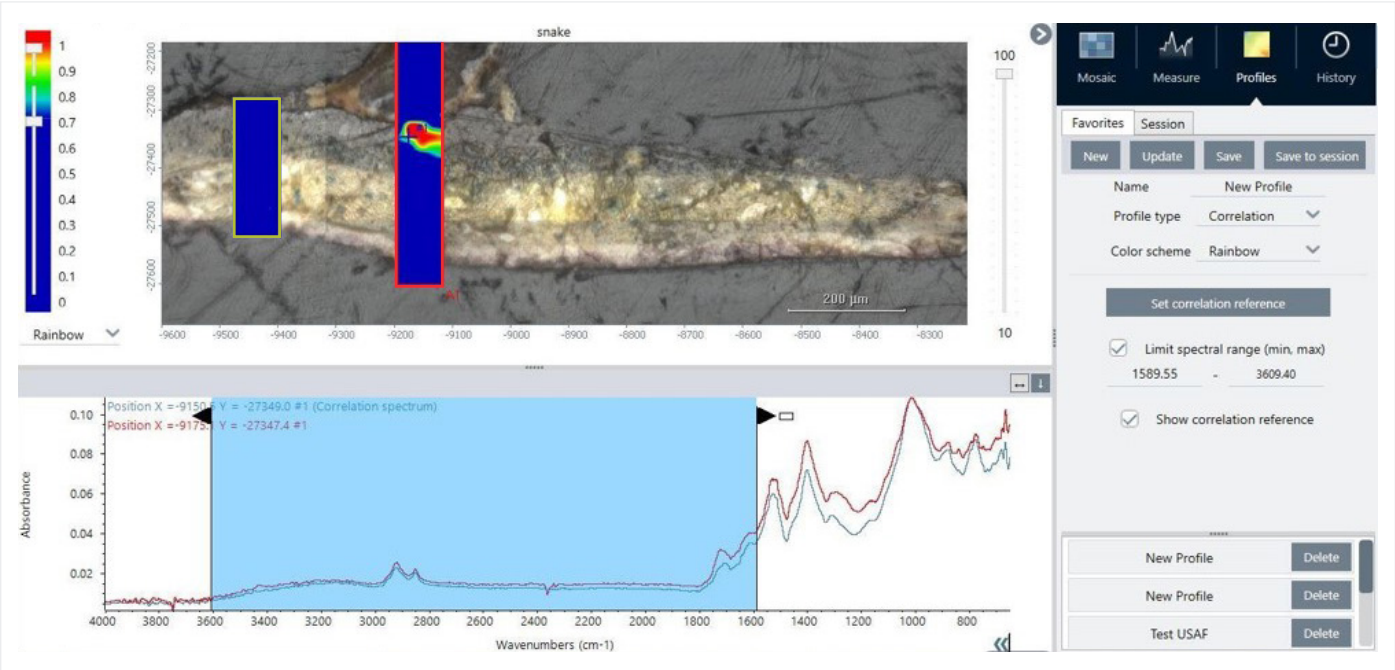

Figure 10. Protein correlation map, with a heatmap showing the presence of proteins.

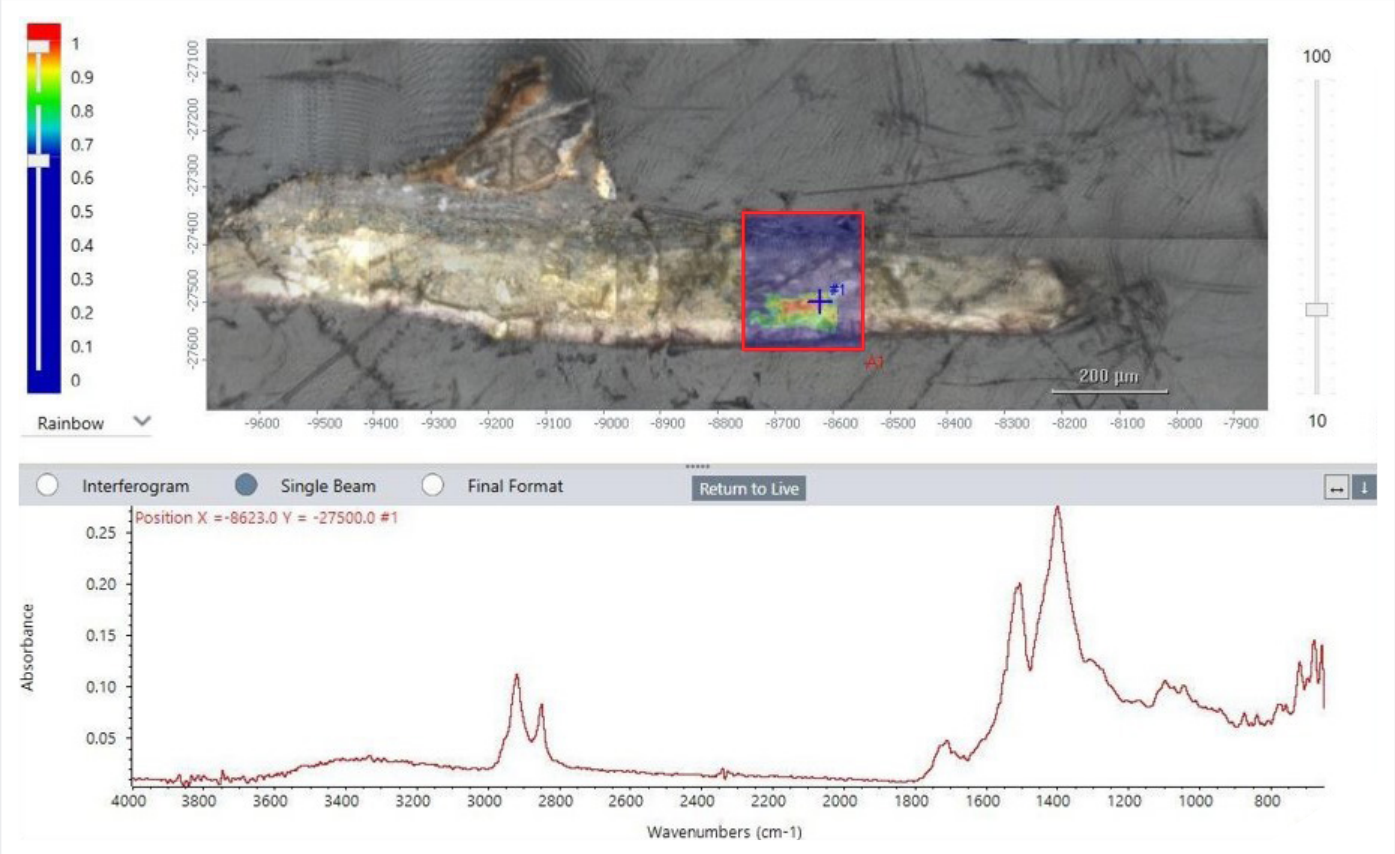

Figure 11. Oil correlation map including ATR data. The heatmap in the red box indicates where oils are present.

Oil correlation map including ATR

Figure 11 shows the presence of oil in the pictorial film. The use of oil allowed Tintoretto to easily spread paint, resulting in more vibrant colors, especially when using lacquers or pigments made of precious materials.

Spectra acquired in the regions containing protein also showed signs of other components such as pigments and oils. Using the multicomponent search function in OMNIC Paradigm Software, it was possible to easily identify all of these additional compounds without the need for any further data collection.

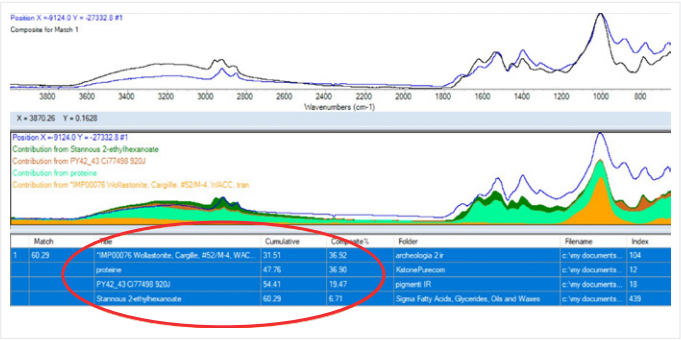

Figure 12. Multicomponent search function in OMNIC Paradigm Software.

Azurite correlation map

The correlation map in Figure 13 shows the presence of azurite, which was corroborated by copper signal in the SEM-EDS analysis. Tintoretto reserved the use of important and expensive pigments for the decoration of small parts. To vary the intensity of the composition, he played with the size of the pigment grains as well as the application of thin pictorial layers to create vibrant textures.

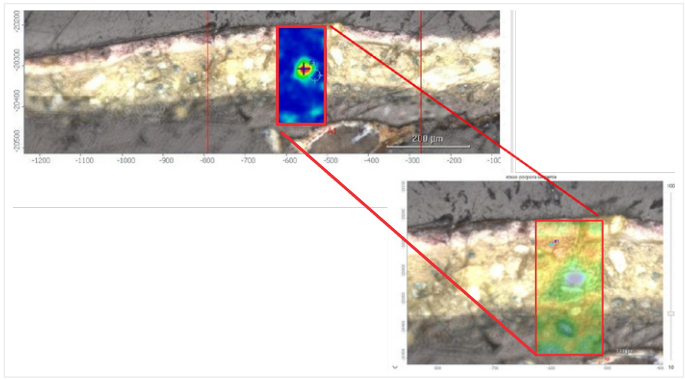

Figure 13. 15x visual map with an overlaid azurite correlation map. The close up clearly shows an azurite grain.

Magnesite correlation map

Correlation maps, corroborated by SEM-EDS analysis, identified the presence of magnesite, which was used as filler to produce vibrant surfaces and reduce the use of precious pigments.

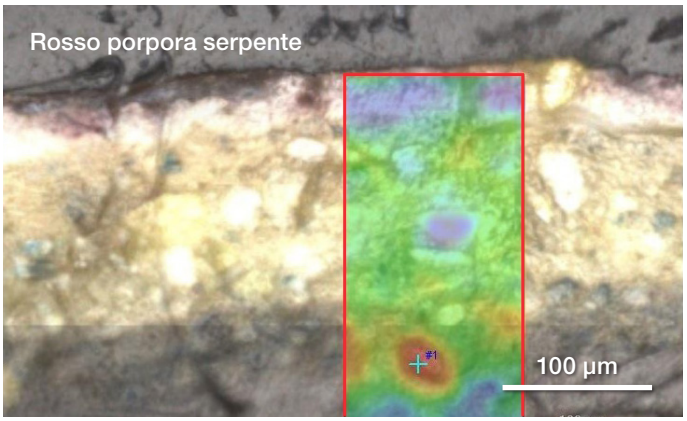

Figure 14. 15x visual map with an overlaid magnesite correlation map; magnesite grains can clearly be seen.

Malachite correlation map

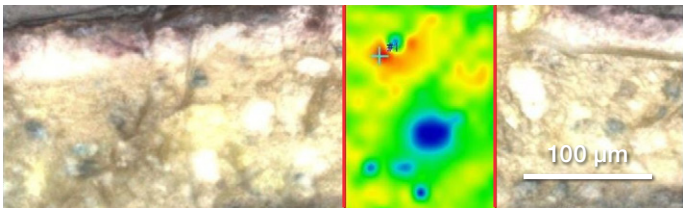

Figure 15. 15x visual map with an overlaid malachite correlation map.

Carbonate correlation map

As identified in the correlation maps, carbonates appeared mainly in the preparation layer. The presence of cerussite is common in all layers and was likely added not only for optical reasons, but also to facilitate and speed up the drying process of the pictorial film.

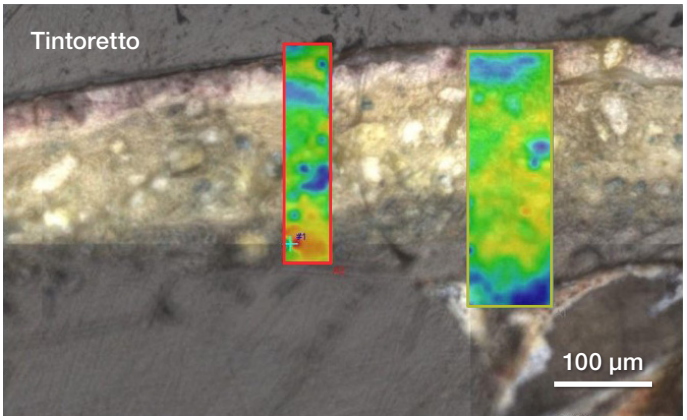

Figure 16. 15x visual map with overlaid carbonate correlation maps.

Conclusions

All materials that were expected to be found in the paint sample were successfully identified using the Nicolet RaptIR FTIR Microscope, combined with the multicomponent search function of OMNIC Paradigm Software. Overall, the following materials and their locations were identified:

- Linseed oil, not only in the upper pictorial film, but also in the preparation layer
- Proteins in animal glue, which are commonly mixed with white lead or earth pigments
- Azurite
- Magnesite
- Malachite
- Calcium and magnesium carbonates

These results were corroborated with SEM-EDS. Overall, this application note demonstrates the versatility and utility of micro-FTIR spectroscopy in the analysis of painting sample cross sections.

References

1. Spring, M et al. 'Black Earths': A Study of Unusual Black and Dark Grey Pigments used by Artists in the Sixteenth Century. *National Gallery Technical Bulletin* 24, pp. 96-114 (2003)
2. Spring M et al. Investigation of Pigment-Medium Interaction Processes in Oil Paint containing Degraded Smalt. *National Gallery Technical Bulletin* 26, pp. 56-70 (2005)
3. Joyce, P and Lorenzo, L. Preliminary observation on the technique and materials of Tintoretto. *Studies in Conservation* 17, pp. 153-180 (1972)
4. Meilunas, RJ et al. Analysis of aged paint binders by FTIR Spectroscopy. *Studies in Conservation* 35, pp. 33-51 (1990)
5. Koller, J and Baumer, U. "Jacopo Tintoretto: the binding media used in his prestezza-art" in Tintoretto: The Gonzaga Cycle. *Hatje Cantz Verlag* (2000)
6. Fumo, G. Tintoretto svelato il soffitto della Sala dell'Albergo nella Scuola Grande di San Rocco. Storia, ricerche, restauri. *Skira* (2010)
7. Tumosa, CS and Mecklenburg, MF. The influence of lead ions on the drying of oils. *Studies in Conservation* 50, pp. 39-47 (2005)

Learn more at **thermofisher.com/raptir**

For research use only. Not for use in diagnostic procedures. For current certifications, visit thermofisher.com/certifications
© 2023 Thermo Fisher Scientific Inc. All rights reserved. All trademarks are the property of Thermo Fisher Scientific and its subsidiaries unless otherwise specified. AN56373_E 01/23M

ThermoFisher SCIENTIFIC

Notes

Learn more at **thermofisher.com/raptir**

thermo scientific

For research use only. Not for use in diagnostic procedures. For current certifications, visit thermofisher.com/certifications
© 2023 Thermo Fisher Scientific Inc. All rights reserved. All trademarks are the property of Thermo Fisher Scientific and its subsidiaries unless otherwise specified. CM56368_E 04/23M